



A01-34489

AIAA 2001-3853

Combustion Research Needs for  
Helping Development of Next-  
Generation Advanced Combustors

H. C. Mongia<sup>1</sup>, J. P. Gore<sup>2</sup>, F. F. Grinstein<sup>3</sup>, E.  
J. Gutmark<sup>4</sup>, S.-M. Jeng<sup>4</sup>, V. G. McDonell<sup>5</sup>, S.  
Menon<sup>6</sup>, G. S. Samuelsen<sup>5</sup>, D. Santavicca<sup>7</sup>,  
and R. J. Santoro<sup>7</sup>

1: GE Aircraft Engines, Cincinnati, OH 45215

2: Purdue University; 3: Naval Research Lab;

4: University of Cincinnati; 5: University of California, Irvine

6: Georgia Tech; 7: Penn State University

37th AIAA/ASME/SAE/ASEE Joint  
Propulsion Conference & Exhibit  
8-11 July, 2001  
Salt Lake City, Utah

For permission to copy or to republish, contact the copyright owner named on the first page.

For AIAA-held copyright, write to AIAA Permissions Department,  
1801 Alexander Bell Drive, Suite 500, Reston, VA, 20191-4344.

## Combustion Research Needs for Helping Development of Next-Generation Advanced Combustors

H. C. Mongia\*<sup>1</sup>, J. P. Gore<sup>2</sup>, F.F.Grinstein<sup>3</sup>, E. J. Gutmark<sup>4</sup>, S.-M. Jeng<sup>4</sup>, V. G. McDonell<sup>5</sup>,  
S. Menon<sup>6</sup>, G. S. Samuelsen<sup>5</sup>, D. Santavicca<sup>7</sup>, and R. J. Santoro<sup>7</sup>

### ABSTRACT

Combustion research activities conducted during the last 30 years have helped increase our fundamental understanding of the various critical processes involved in gas turbine combustors. These along with significant advances in combustion diagnostics have given us good DRA and CCD-based tools for post-diction (anchoring) and identified need for further improving the diagnostic capability and the model accuracy for pre-diction as exemplified in this paper.

### I. INTRODUCTION

Gas turbine combustion system design process and tools have developed progressively over the last 25 years as summarized by Mongia.<sup>1,2</sup> Simple multi-dimensional combustion models (based on the standard k-ε model, deterministic Lagrangian spray model with a 2-step eddy-breakup model, six-flux radiation model) were calibrated (as part of the empirical/analytical design methodology<sup>3</sup>) with measured internal emissions profiles from several can and annular combustors<sup>4,6</sup>. For example, Figure 4 of Mongia, Reynolds and Srinivasan<sup>6</sup> lists four combustors wherein internal emissions profiles measurement were made including:

1. An experimental can combustor of 5-inch diameter. Radial profiles of CO<sub>2</sub>, CO and NO<sub>x</sub> were made inside the combustor up to 10 atmospheres with both natural gas and Jet-A fuels.
2. Internal profiles of CO, CO<sub>2</sub> and NO<sub>x</sub> were measured on the two production engine reverse-flow annular combustors (the TFE731-2 and UT76) at ambient pressure with heated inlet air temperature.
3. Similarly on an axially-staged reverse-flow annular combustor of NASA sponsored Pollution Reduction Technology program for small engines.

\* Copyright © 2001 by the authors. Published by AIAA with permission.

1. GE Aircraft Engines
2. Purdue University
3. Naval Research Lab
4. University of Cincinnati
5. University of California at Irvine
6. Georgia Institute of Technology
7. Penn State University

Approximate as these measurements might have been, they provided useful insight for CCD (computation combustion dynamics) models and their application in the combustor design process – so-called empirical/analytical design methodology.

The next phase of CCD model validation was conducted under the NASA sponsored Hot-Section Technology Aerothermal Modeling Phase 1 (Reference 7) where several “benchmark” quality test cases (see Figures 16, 17 and 18 of Reference 8) were run to assess the accuracy of the state-of-the-art models. These test cases included:

1. Simple flows
2. Complex non-swirling flows
3. Complex flows with swirl.

In parallel with HOST Phases I<sup>7</sup> and II<sup>9, 10</sup> continued LDV-based diagnostic investigation and the attendant model validation on a selective basis; e.g., refer to Figures 14 and 15 of Reference 8. In parallel with these applied research activities has been happening a revolutionary change in the combustion design concepts as described in Section 2.

The first extensive systematic collection of bench-mark quality data took place under the NASA sponsored HOST Phase II Aerothermal modeling as summarized in Section 3. The follow-on joint activities are described in Sections 4, 5 and 6 with the selective universities with more emphasis on understanding the critical process occurring in “production” combustor subcomponents. This has laid a strong foundation for moving on to the next step as explained in Section 7. The research community is being asked to work closely with GEAE’s combustion designers to achieve the following “bottom-line” objective:

Conduct fundamental investigations, develop accurate CFD-based models that combustion designers can use with confidence to analytically design next-generation gas turbine combustion systems without requiring the supporting rig testing/verification process, a common current practice. Instead, the designer is being challenged to use the engine testing only for the sole purpose of design substantiation.

## II. Evolving Combustor Technology

Figure 1 presents a typical schematic of a conventional turbo-propulsion engine combustor cross-section with airflow distribution<sup>11</sup>, as well as a dome with 12 to 30 piloted airblast nozzles, each concentric with a set of co-rotating swirlers.

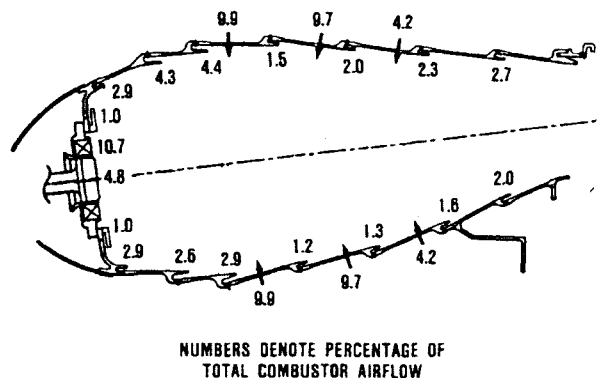


Figure 1: Typical small turbo-propulsion engine combustor with typical airflow distribution.

Even though several unsolved problems remain for the single swirler plus its interaction with fuel injectors for simple gas turbine combustors as shown in Figure 1, the designers have moved on to more complex fuel/air mixing devices as necessitated by the design requirements. Consequently, the modeling and advanced diagnostics activities have also moved on to investigate these design-driven complex mixers, as discussed in the following paragraphs.

GEAE has developed a unique fuel/air mixer called swirl cup that is used in several of its gas turbine engines, Figure 2. A typical swirl cup comprises of a pressure atomizer that is surrounded by two counter-rotating swirling streams in addition to purge air for the primary swirler and flare air for the cup. This mixer has been studied extensively, as summarized by Mongia et al<sup>12</sup> The airflow rate through the swirl cups ranges typically between 17% through 22% compared to 15.2% shown for the combustor of Figure 1.

Joshi et al<sup>13</sup> describe the LM6000 Dry Low Emission combustor (DLE), as shown in Figure 3. The combustor has three domes arranged radially to permit parallel staging of the three domes. The middle and the outer domes each consist of 30 premixers while the inner dome has 15. The domes of the combustor are protected from the hot combustion gases by segmented heat shields.

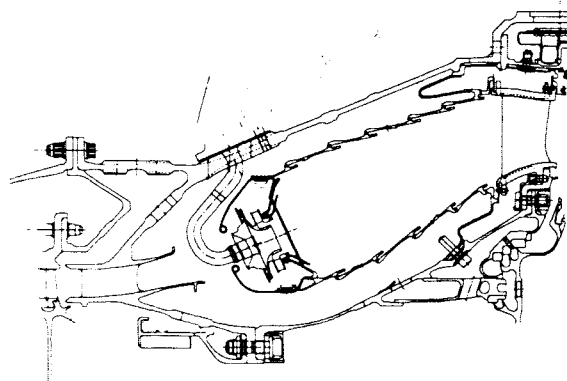


Figure 2: A rich swirl cup based single annular combustion system.

The 75 heat shields which utilize advanced cooling technology also protect burning domes from the quenching effects of air in non-burning domes during staged operation permitting the combustor to operate lean premixed from light-off to full power. Spent cooling air from the heat shield is directed away from the flame stabilization zones permitting the combustor to operate at leaner fuel-air ratios. Turbine nozzle cooling air is utilized to cool the liners convectively on the backside. Two cooling nuggets like the ones used on aircraft engine CF6-80C2 (parent engine of the LM6000) are used at the aft end of the liners to trim the temperature profile entering the turbine nozzle.

The 75 premixers are arranged on 15 two-cup and 15 three-cup assemblies. The two-cup assemblies do not have the innermost premixer. The removable premixers utilize the Dual Annular Counter-Rotating Swirlers (DACRS) premixer shown schematically in Figure 4. The DACRS premixer comprises of two axial counter-rotating coaxial swirlers (recall two counter-rotating swirlers used in swirl cups) mounted with a hub separating them followed by a mixing duct. The inner swirler has a centerbody along the premixer and the mixing duct. The centerbody is conical in shape and ends in a point at the exit end of the premixer. A small amount of air is allowed to pass through the centerbody to eliminate the small recirculation zone that could form at its aft end. Fuel is injected from holes drilled into the hollow outer swirler vane.

Selective DACRS premixers have features to ameliorate combustion dynamics. A small amount of fuel (typically 10%) is injected into the combustor from holes in the walls of the mixing duct. This feature for Enhancing Lean BlowOut (ELBO) is shown in Figure 4.

Fuel injected from the ELBO holes increases the local fuel air ratio in the mixing region between recirculating burnt gases and fresh incoming mixture. The ELBO feature also provides axial staging of the fuel. The increased fuel air ratio in the mixing region along with axial staging helps to decouple any fuel injection related acoustic coupling

mechanisms. A similar feature also exists on the outer dome pre-mixers

Several advanced technology combustors have been demonstrated that are distinctly different from those presented in Figures 1 through 3. Some of these are described in the following paragraphs.

Figure 5 shows a cross-section of a mixer designed for a stoichiometric segmented ceramic combustor<sup>8</sup>. This mixer consists of two small co-rotating swirlers around a pressure swirl atomizer. The inner swirler is intended for air-assisting the pressure atomizer for improving the spray quality in addition to providing air for keeping the tip free of carboning. The outer swirler and a third counter-rotating swirler provide high-shearing streams for atomizing the thin fuel film. These along with the dome-mounted fourth counter-rotating swirler provide a highly turbulent

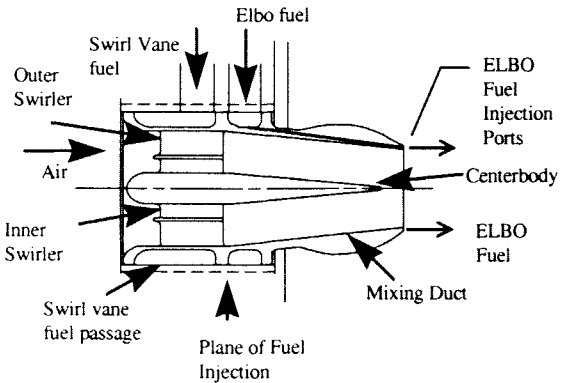


Figure 4: LM6000 DLE mixer- Dual Annular Counter-Rotating Swirlers (DACRS).

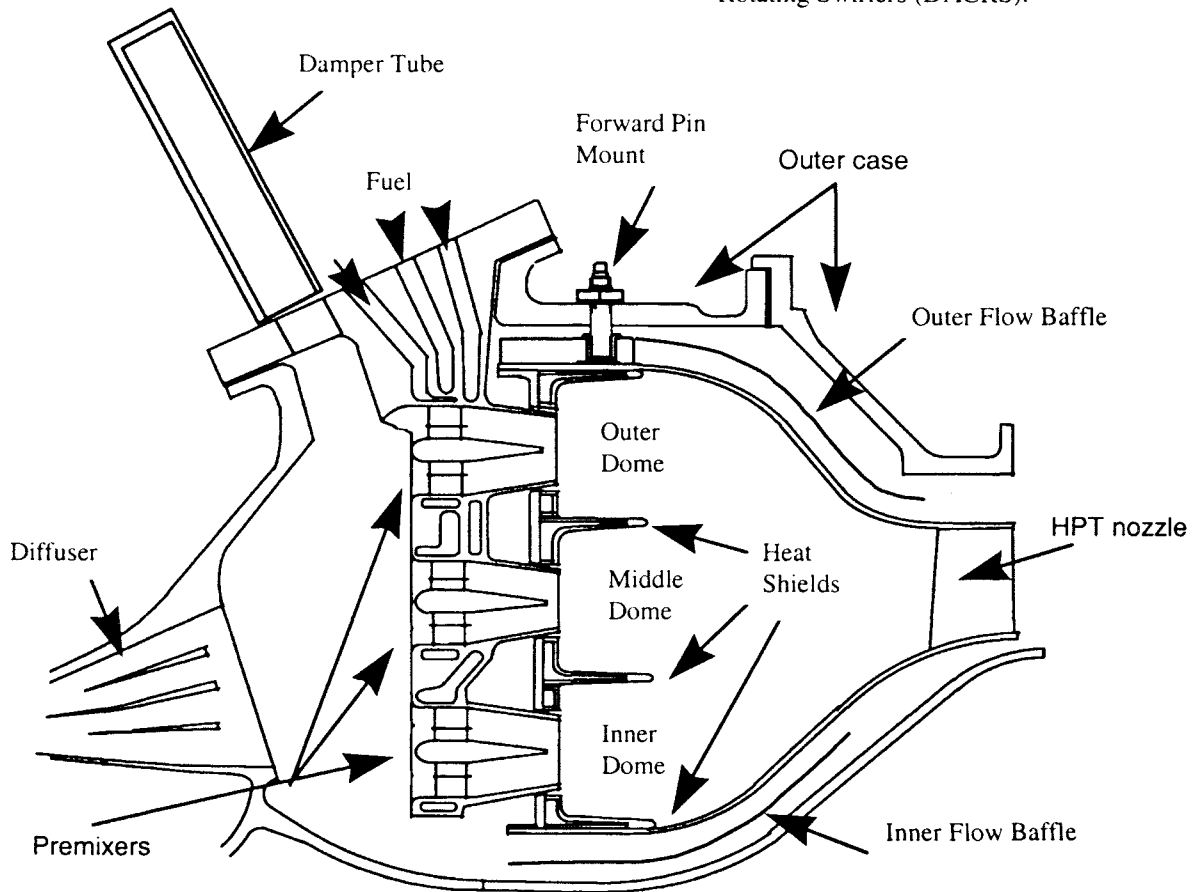


Figure 3: LM6000 Dry Low Emissions combustion system.

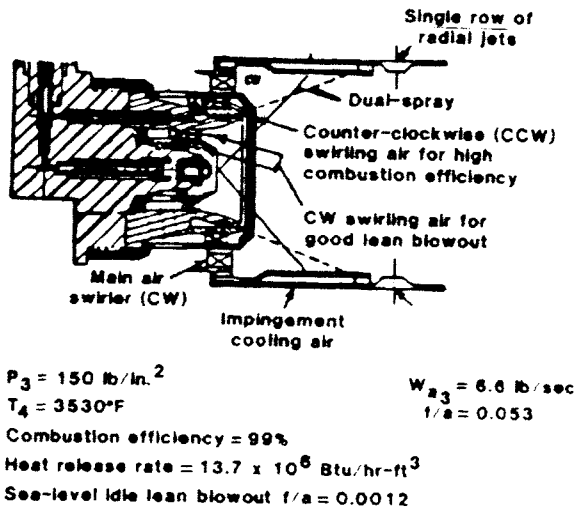


Figure 5: A 4-swirler mixer for stoichiometric combustor application.

well-mixed fuel/air mixer that combined with impingement/film cooled stream and a single-row of primary jets have provided a unique flow-field for the stoichiometric combustor with excellent sea-level idle operation.

Two other advanced mixers are shown in Figure 6. One mixer used a piloted airblast nozzle that is surrounded by 2 co-rotating axial swirlers<sup>14</sup>. The other mixer used co- and counter-rotating set of four swirlers with cross-stream liquid plane jet injection<sup>15</sup>. The former had 64%  $W_{a36}$  through the dome whereas the latter had all the combustor air flowing through the dome at the design point. The first mixer and the combustion system was successfully operated for 2400 F  $\Delta T$  operation whereas the second was for a regenerative automotive gas turbine application.

### III NASA HOST Phase II Studies

The UCI research group under the guidance of McDonell and Samuelsen, and the Purdue team supervised by Sullivan and Murthy undertook an extensive LV-based characterization of the flow field established by a typical engine combustor dome swirler of 60° vane angles. Their results are summarized in References 9 and 10 along with validation of the state-of-the-art turbulence models. There are several unique aspects of these studies including the following:

- Extensive benchmark quality data appropriate for a real combustor hardware
- A building-block approach starting with the relevant simple flows ending eventually with the characterization of the complex flow field for "production" swirlers and fuel nozzles. This included single round jet, co-axial jets, annular jet with a center

disk, swirler with a disk, and a short filming airblast nozzle, as shown in Figure 7.

- Well-defined inlet conditions for swirlers and primary holes. Figure 8 shows the elements of the 5-cup rectangular test rig used by Sullivan, Murthy and their students at Purdue University for studying the interaction between the dome swirlers and primary jets.
- The model validation effort<sup>9,10</sup> clearly showed the limitations of the CFD capabilities as well the inadequacy the turbulence models including the standard and modified k- $\epsilon$  models, and the full Reynolds stress transport model.
- This modeling effort showed once again that the current k- $\epsilon$  model based formulation as well as the state-of-the-art full Reynolds stress model did not capture the finer details of the flowfield accurate enough for relying completely on the combustor analytical design process. Instead, one should continue to use combined empirical/analytical design process including the most recent approaches, namely hybrid modeling and/or anchored methodology.

However, significant advances have since been made in the CFD and modeling areas. This therefore leads to the second round on the use of CFD tools and advanced turbulence models.

### IV PSU and UIUC Fundamental Studies

Although a lot still needs to be done for simple swirlers and pure airblast nozzles similar to the configurations studied under NASA HOST's sponsorship, the combustor designed for modern low-emissions and/or high-performance gas turbine engines have relatively more complex fuel air mixers. A number of recent fundamental investigations have therefore been focused on studying these advanced devices as described briefly in this section and the two sections that follow.

An outstanding example of recent reacting flow investigations with emphasis on combustion dynamics is by Santoro, Santavicca<sup>16</sup>. They studied dynamic characteristics of two mixers, namely PSU mixer and a generic 1X DACRS mixer. The study included the effects of combustor length, equivalence ratio, inlet pressure and temperature on the combustor's operating regimes. The phase-resolved measurements of the energy release process (through chemiluminescence and planar laser-induced fluorescence, PLIF techniques) relative to combustion pressure oscillation provided detailed understanding about the coupling mechanism between heat release and pressure oscillations.

Concurrently, Peters, Lucht and their students at University of Illinois at Urbana-Champaign (UIUC)

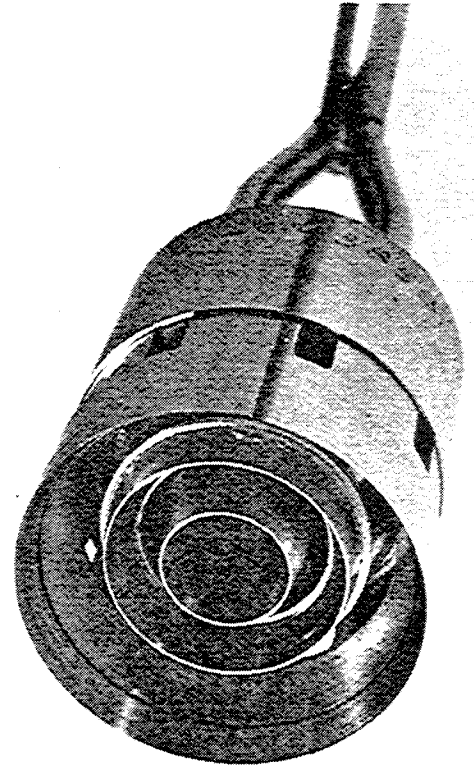
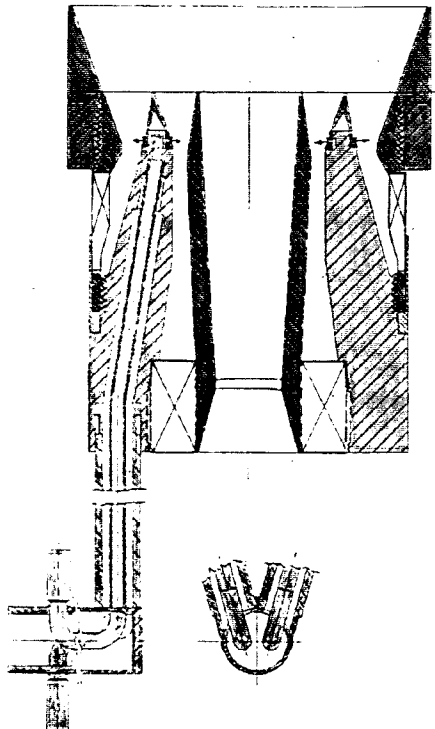
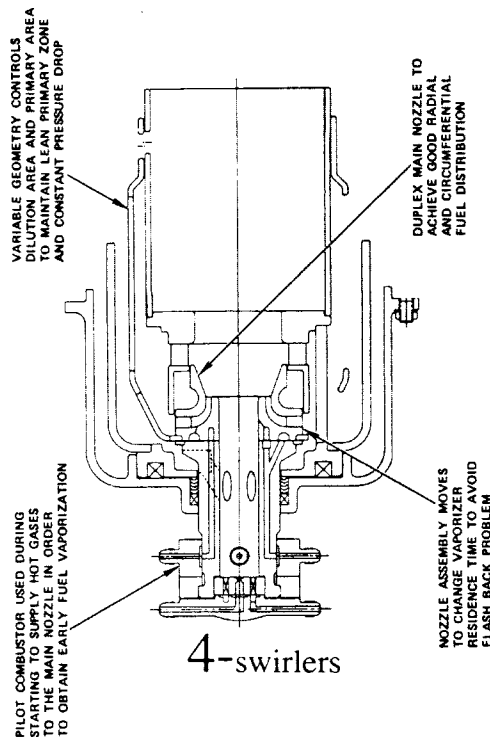
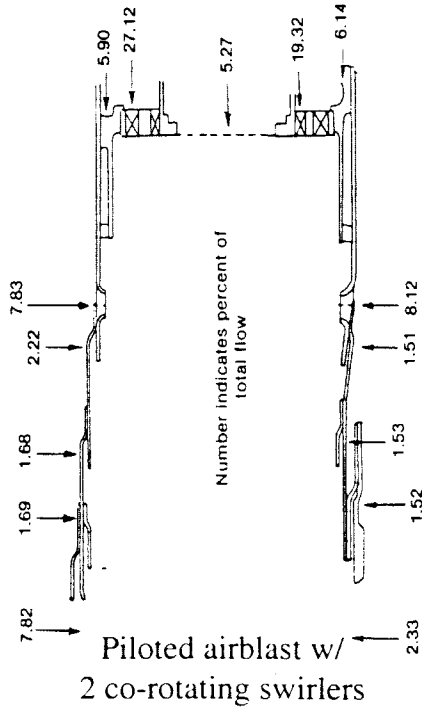


Figure 6: Two typical high-dome flow technology combustors for high  $\Delta T$  propulsion, and regenerative automotive gas turbine applications.

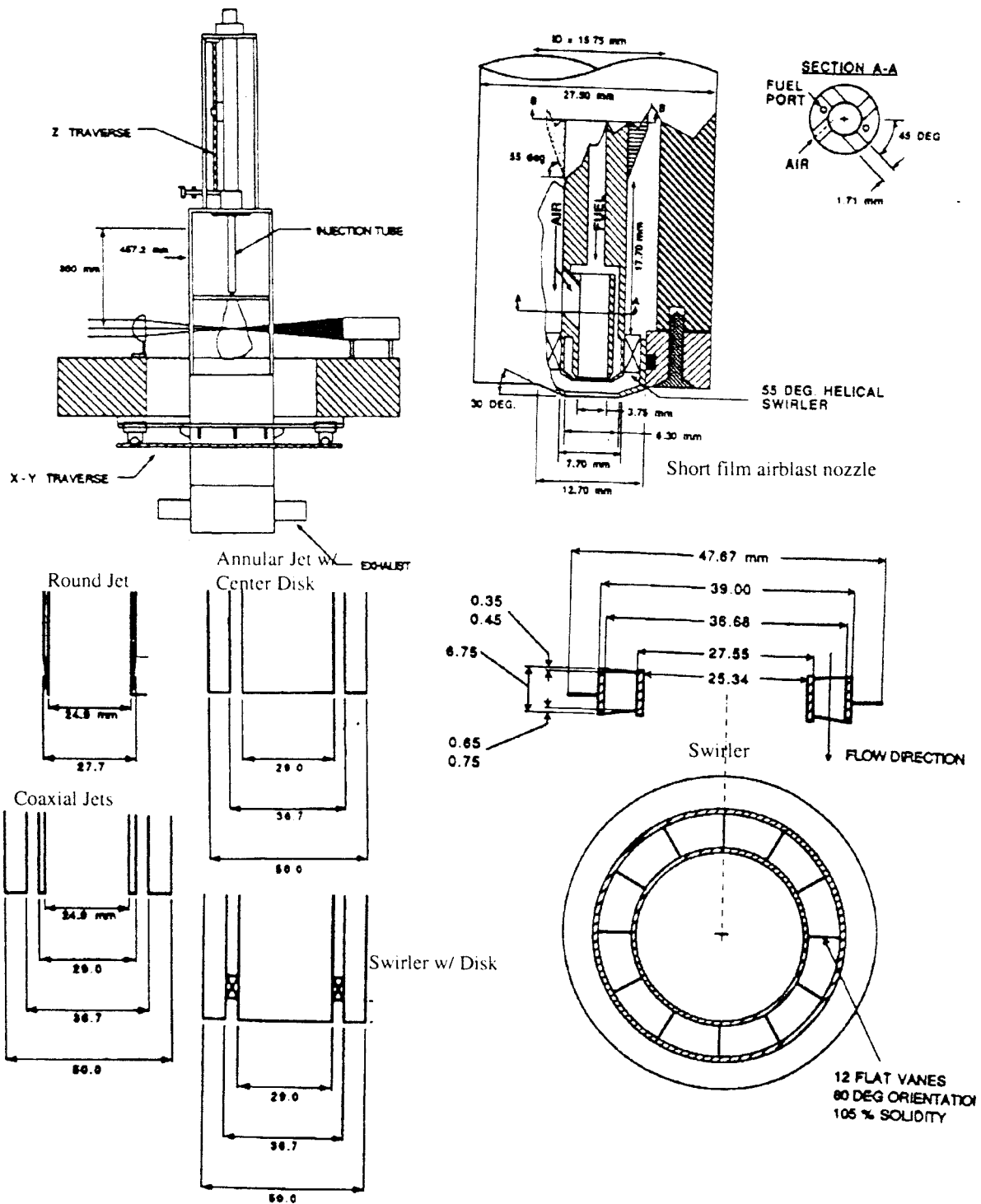


Figure 7: LV/PDPA 2-D axisymmetric measurements sponsored by NASA HOST

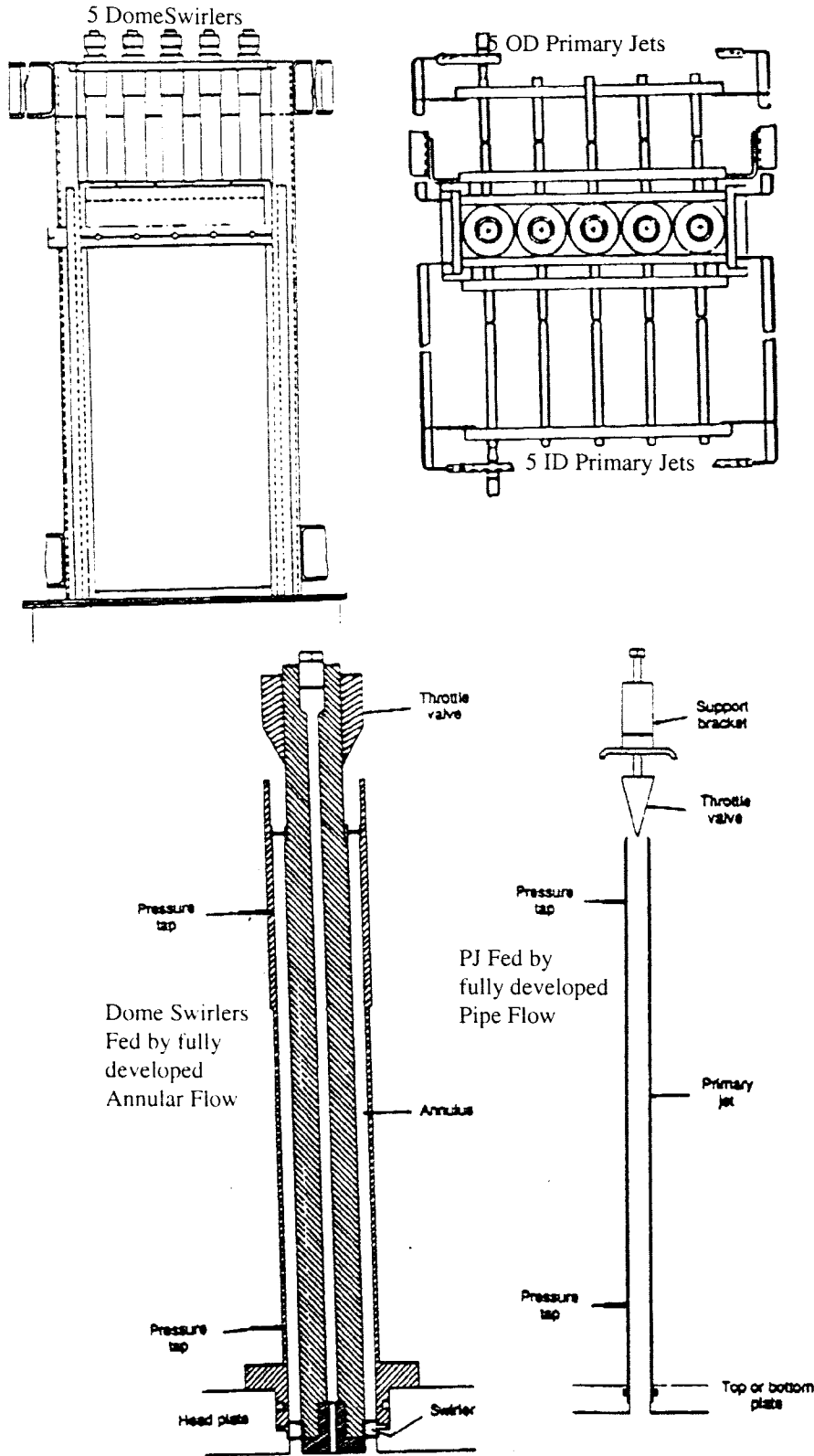


Figure 8: LV measurements on a 5-cup rectangular sector sponsored by NASA HOST used acetone PLIF imaging to determine the level of mixing as a function of DACRS mixer geometry as influenced by equivalence ratio, airflow rate, inlet temperature and pressure. The flame structure was studied

by using OH PLIF imaging technique. Their work clearly showed that the generic DACRS mixing field is dominated by large-scale structures.

A typical natural gas (NG)/air mixer and combustor can comprise of a single swirler on a hub followed by a constant height annulus into which NG is injected cross-stream and allowed to mix before discharging into a dump combustor. Such an idealized set-up shown as the PSU's mixer and set-up shown in Figure 9, is not untypical of some of the low-pressure DLE/DLN engine combustors<sup>17</sup>. The PSU swirler has 8 straight flat vanes with a 45°-vane angle. The swirler is located 38 mm upstream of the dump plane as shown schematically in Figure 10. The swirler hub diameter is 9.53 mm. NG fuel is injected into the annulus through ten 0.75 mm diameter holes at an axial location,  $X_{inj}$  (= 36.8 mm), upstream the dump plane. The combustor diameter and length are 45 mm and 235 mm, respectively, giving  $L/D = 5.22$  compared to typical 2.0 to 3.0 in gas turbine can combustors.

A cross-section of the PSU test rig used for the DACRS 1-X model is shown along with that of the University of Illinois rig for the 3-X DACRS, Figure 11.

The generic DACRS mixer studied by PSU and UIUC comprise of:

1. 10 outer swirler vanes of 45-degree twist with inlet OD of 0.938 inches (for 1X)
2. 5 counter-rotating 55-degree vanes with inlet OD of 0.55 inches
3. A center-body starting at the inlet with 0.241-inch diameter and reducing to a "point" at  $X = 1.391$  inches
4. 3 fuel injection points on the trailing edge of each of the 10 outer swirler vanes plus one additional through the outer mixer wall located in-between the vanes.

5. A conical mixing section with exit diameter of 0.632 inches (for 1X) and area convergence of approximately 2.2.

The mixer exit diameters are 16 mm (for 1X scale) and 48 mm for 3X scale DACRS.

The advanced diagnostic studies by Lucht and Peters on the 3X scale mixer showed:

1. Significant time-averaged spatial variations (near the mixer exit plane) in the mixture's equivalence ratios dissipated quickly further down stream. For example at 12-mm downstream from the mixer exit (=0.25 times mixer exit diameter,  $D_{mixer}$  or 0.1 combustor can diameter,  $D_c$ ), local maximum  $\phi$  ( $\phi_{max}$ ) is 1.51 times average  $\phi$  ( $\phi_{avg}$ ) of 0.7 when mixer pressure drop ( $\Delta P$ ) is 3%. However, when  $\phi_{avg}$  is decreased to 0.4 or  $\Delta P$  is increased to 5%,  $\phi_{max}/\phi_{avg}$  reduces to 1.3 and 1.24, respectively.
2. An order of decrease in time-averaged spatial variations within an axial distance of  $1.5D_{mixer}$ .
3. Even more temporal variations exist, by approximately a factor of 3 at the first axial plane, 12 mm downstream from the mixer exit,  $0.25 D_{mix}$ . The persistence of the temporal variations exists for a long distance downstream in the combustor..
4. The flame structure was dominated by large-scale structure with significant temporal variations consistent with non-reacting mixing studies. For the flames with 0.6 average (lean blow-out  $\phi = 0.55$ ) these temporal variations can be seen separating and creating isolated flame pockets, as evident from the time-resolved OH PLIF signals.

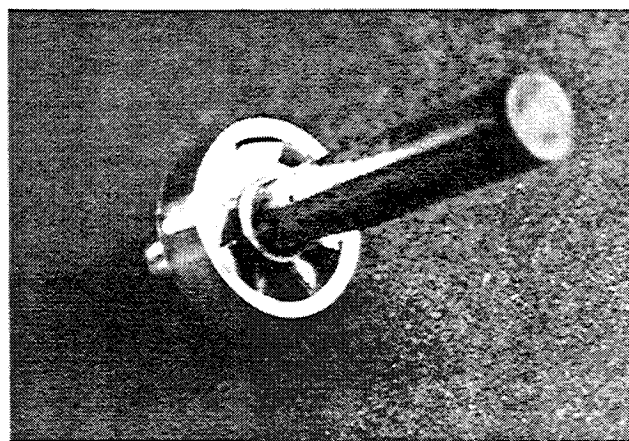
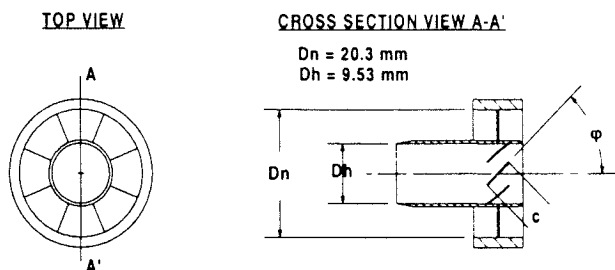
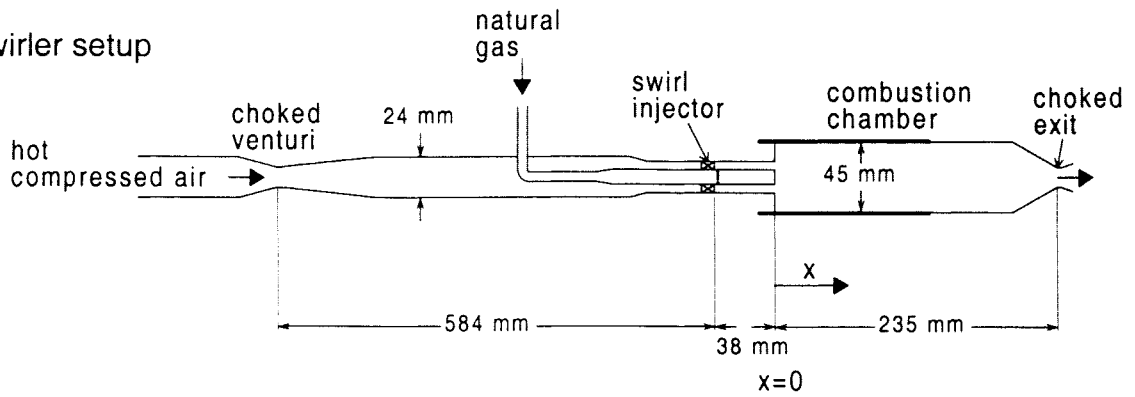
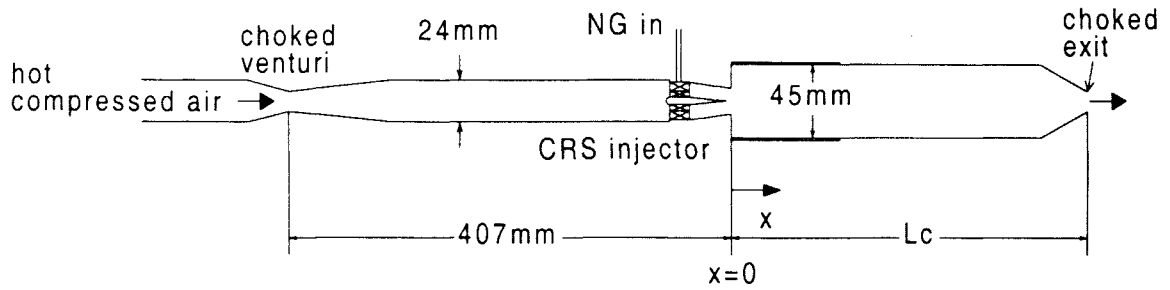


Figure 9: Single swirler mixer (PSU mixer) investigated by Santoro, Santavicca and their associates.

Single swirler setup

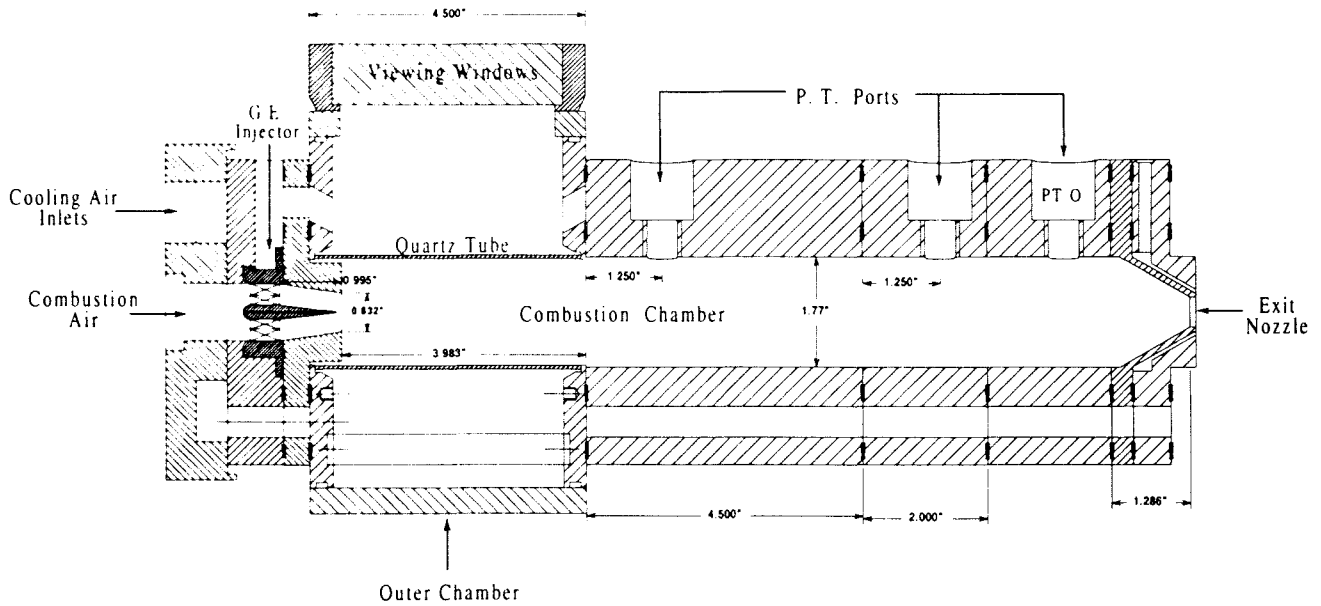


Generic DACRS setup

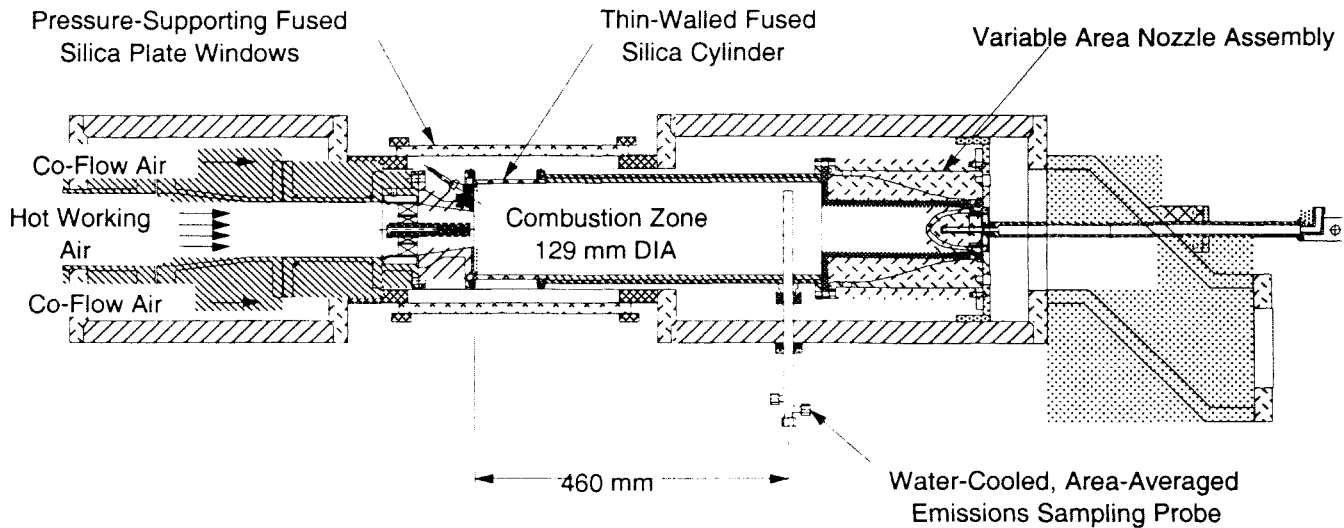


$L_c = 235\text{mm or }350\text{mm}$

Figure 10: PSU test rigs for dynamics investigation of single swirler and generic DACRS mixers.



(a) PSU test rig for conducting dynamic investigation on 1-X generic DACRS mixer



(b) University of Illinois test rig for conducting mixing study on 3-X generic DACRS mixer

Figure 11: Experimental test rigs for fundamental investigation on generic DACRS mixers.

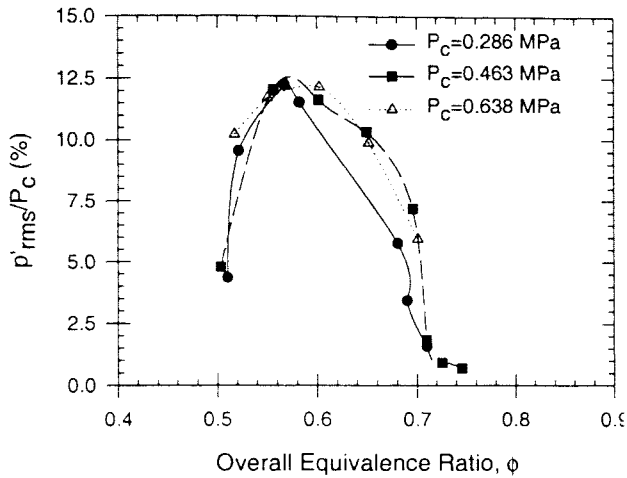
- The average location of the flame front is at the edge of the mixing duct. It appears that the primary mechanism that determines the location where the reaction front closes is vortex breakdown, which begins to occur several centimeters downstream of the premixer exit. The low OH signal strength along the centerline of the duct indicates the absence of reaction near the centerline and the surrounding region. What happens to the mixing processes, vortex breakdown, flame anchoring and the reaction near the center as one increases  $\phi$ , inlet pressure and temperature? How dynamics are impacted by making changes in the mixer geometrical features (including vane angles, flow splits, number and size of the fuel injection holes)? Answering these questions and many other relevant issues would make an excellent research study.

The UIUC study clearly shows that the turbulent structure can not possibly be captured accurately by the Reynolds Averaged Modeling Approaches (RAMA – a state-of-the-art practice) especially if one were to achieve the accuracy and reliability levels of the models comparable with that of experimental data. Moreover, the acoustic heat release interaction processes are indeed too complex to be captured by RAMA. Affordable and accurate large eddy simulation techniques need to be formulated, developed and validated for the low-emissions and/or high-performance engine combustors.<sup>18-20</sup>

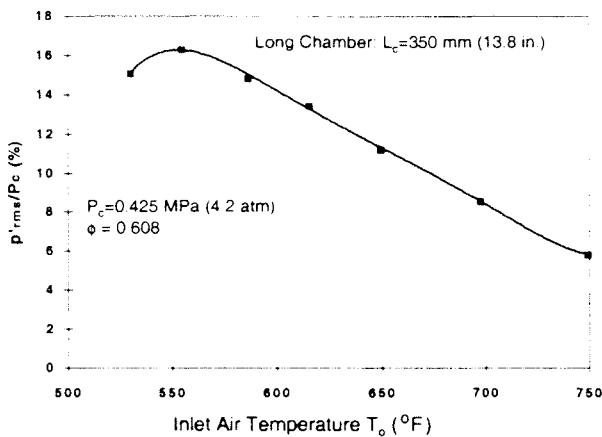
The major objective of the combustion instability study conducted by Santoro, Santavicca and their associates<sup>16</sup> was achieved in that an extensive set of detailed

measurements of the stability characteristics of the DACRS injectors under well-controlled conditions was obtained. A data set representing the stability behavior over a wide range of conditions resulted that specifically addressed injector stability behavior as a function of equivalence ratio, inlet air temperature, pressure and chamber configuration. Additionally, phase-resolved measurements of the energy release process with respect to the observed pressure oscillations were obtained from global and spatially resolved measurements using chemiluminescence and planar laser-induced fluorescence techniques. These measurements provided detailed understanding as to the coupling mechanisms between heat release and pressure oscillations that were observed during unstable operation. Analysis of the data allows evaluation of the role of mechanisms responsible for the initiation and sustenance of the combustion instability including the fluid mechanic effects of swirl, the role of fuel-air unmixedness and fuel feed system coupling. Both the data and these mechanistic insights provide a rich data set from which to develop and validate models intended to describe combustion instability in gas turbine combustors. Details are provided in Reference 16, brief description is given in the following paragraphs.

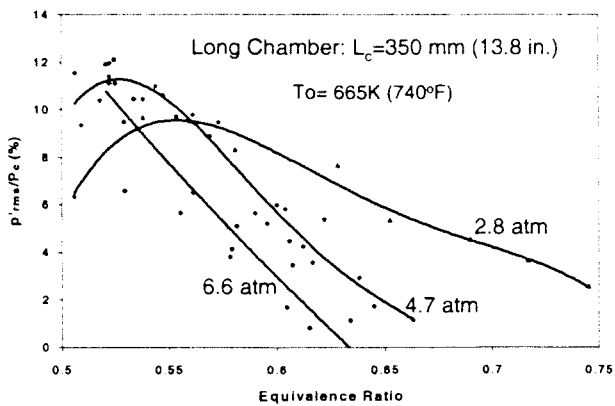
Figures 12 (a), (b) and (c) present measured combustion pressure oscillations, RMS values ( $p'_{rms}$ ) normalized by average combustion chamber pressure ( $P_c$ ), as a function overall equivalence ratio, combustor inlet temperature ( $T_o$ ) for different combustion chamber pressures, for the PSU mixer as shown previously in Figure 9. For the given combustor length (of 350 mm (13.8 inches)), the maximum dynamics levels can be function of equivalence ratio as well as inlet temperature; see Figures 12 (a) and 12(c). For a constant equivalence ratio, e.g., 0.608



(a) Relative magnitude of dynamic pressure as a function of equivalence ratio



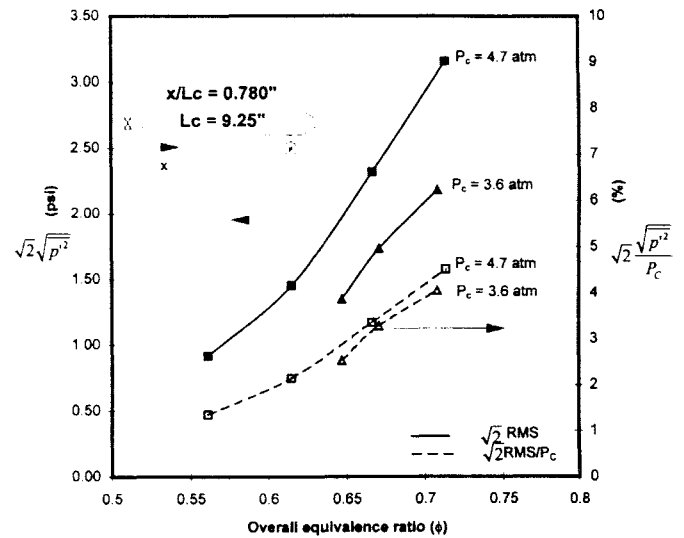
(b) Relative magnitude of dynamic pressure as a function of mixer inlet temperature



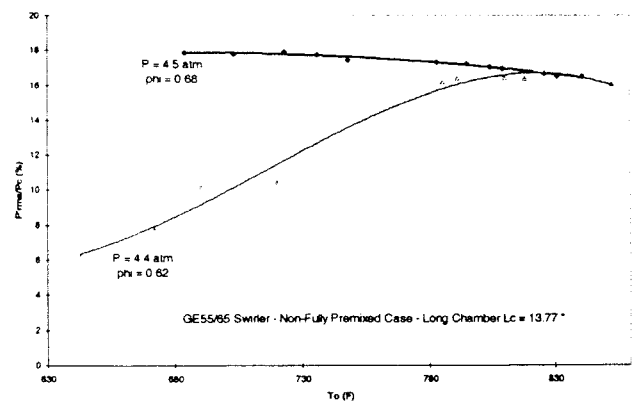
(c) Relative magnitude of dynamic pressure as a function of mixer equivalence ratio for different chamber pressures  
Figure 12: Single swirler mixer (PSU mixer) dynamics results.

as shown in Figure 12 (b), the peak dynamics occur at lower levels of inlet temperature.

Figures 13(a) and 13(b) show the measured impact of combustor lengths (235 mm and 350 mm) for two generic DACRS geometries. For one geometry, the inner swirler/outer swirler vane angles are 45° and 55°, respectively, denoted as 45°/55° in Figure 13 (a). The second geometry has the corresponding 55° and 65° vane angles, denoted as 55°/65° in Figure 13(b). Comparing Figures 12 and 13, it is very easy to conclude that the PSU and DACRS mixers' characteristics are significantly different.



(a) Relative magnitude of dynamic pressure as a function of mixer equivalence ratio for different chamber pressures for short-length combustor [235 mm (9.25 in.)] length with 45°/55° DACRS swirlers



(b) Relative magnitude of the dynamic pressure as a function of mixer inlet temperature for 1X 55/65-deg. DACRS in longer [350 mm (13.77 inches)] tube.

Figure 13: Dynamics of generic DACRS effect of geometry and combustor length.

It may be noted that combustion burning lengths for the three domes of the LM6000DLE are respectively, as compared to 9.25 and 13.77 inches combustor lengths tested in the PSU rig. It should also be noticed that the design pressure and inlet temperature of the LM6000DLE are approximately 30 atmospheres and 1000 F (811K), respectively.

Since only relatively weak instabilities were produced for the DACRS injectors with the short chamber ( $L_c=235$  mm), it was decided to install a longer chamber ( $L_c=350$  mm) and study the effect of chamber length on the instabilities. This longer chamber produced, indeed, drastically different instabilities and flame characteristics with the following general trends.

As shown in Figure 13 and 14 for both DACRS injectors, the flame in the longer tube becomes unstable if the inlet air temperature  $T_o$  is higher than a threshold value  $T_{omin} \cong 672$  K (750°F) and if the equivalence ratio  $\phi$  is greater than  $\phi_{min} \cong 0.59$ . If those two conditions are not met simultaneously, the flame will usually remain stable. The stability maps for both swirler configurations for the DACRS injectors are quite similar, with that for the

55°/65° swirler being slightly shifted towards leaner conditions. Both curves show very high maxima with respect to amplitudes of the observed combustion instabilities (18% rms of the chamber pressure  $P_c$ , i.e. more than 25% absolute amplitude). At higher values of  $\phi$ , the instabilities become weaker but are still substantial. Another important trend is that the instabilities die out at the leanest conditions well before LBO, which typically occurs around 0.48-0.50. This is particularly interesting to note since combustion instabilities are commonly thought to occur (or at least worsen) towards the leanest conditions. Other interesting behavior is the observed impact of the degree of mixedness on the acoustic characteristics as shown in Figure 14. Fully premixed flame is acoustically less active than partially- premixed, identified as non-fully premixed in Figure 14. Further insight on combustion dynamics characteristics of DACRS mixer will ensue by conducting more experimental work at GEAE under higher P3/T3 conditions, in addition to modeling work by Menon, Yang and Grinstein.

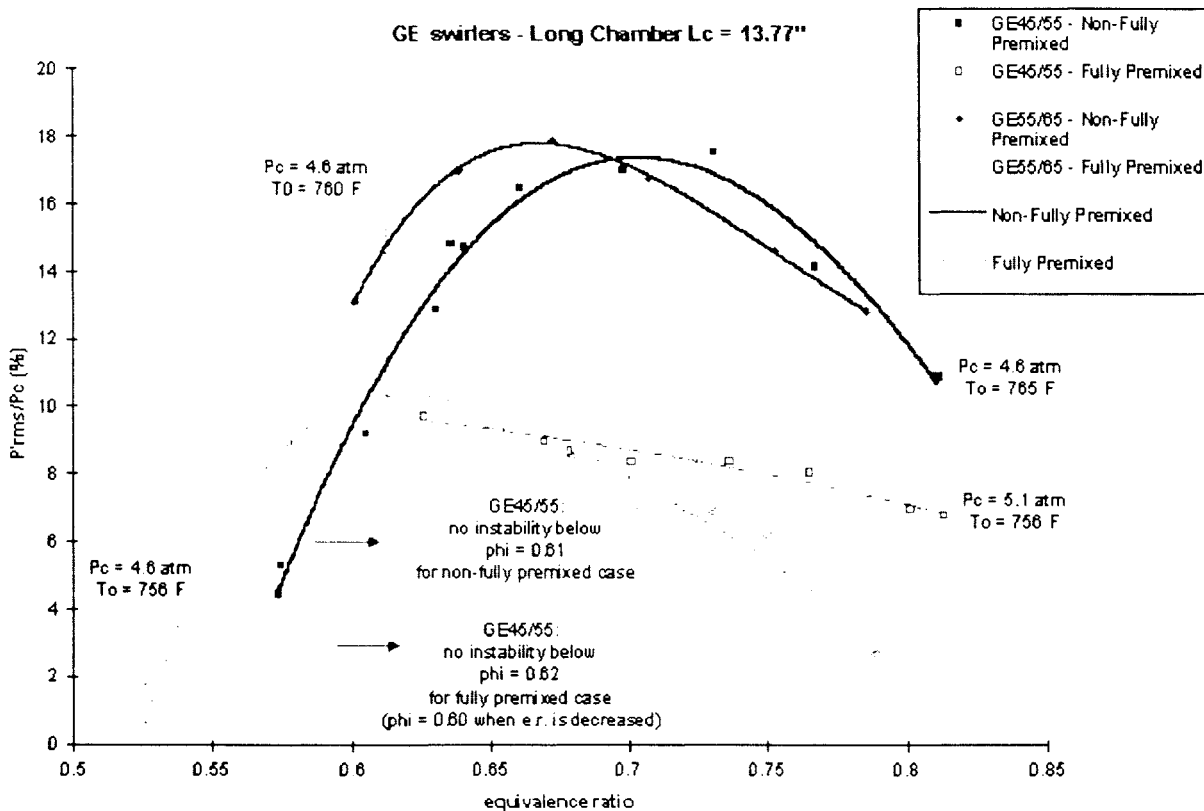


Figure 14 : Combustion Dynamics of generic IX DACRS mixers in a longer combustor can (13.77 inches) is worse than that in shorter cans (9.25 inches).

## V. Purdue and UCI Fundamental Studies

The UCI combustion group led by Samuelsen and McDonnell, and UC activities by Jeng have provided considerable insight on the complex flow field and spray characteristics of typical swirl cups. Some of these studies are summarized in Reference 12. In the following paragraphs, we will summarize recent studies by McDonnell and Samuelsen (as described in detail in Reference 16) relevant to the study reported by Ji and Gore<sup>21</sup>. The main message from these works is:

The flowfield characteristics of complex mixers are significantly different from that of a single swirler.

### Purdue Experimental Apparatus

The flow field at the exit of a premixer module formed by mounting a converging diverging nozzle on a swirler assembly is studied, Figure 15. Single and double radial and axial swirler modules with different vane angles can be mounted in this arrangement. The swirler assembly is fed by air from a plenum chamber. Fuel is added through multiple openings in the incoming airflow. The present measurements are restricted to the flow field without combustion.

### Purdue Particle Imaging Velocimetry System

The incoming airflow is seeded with 1  $\mu\text{m}$  mean diameter  $\text{Al}_2\text{O}_3$  particles using a specially designed fluidized bed, reverse cyclone swirler. A central plane in the nominally axisymmetric flow is illuminated with a laser sheet from a Nd:YAG laser. The Mie scattering from the particles of two closely timed pulses of the Nd-YAG laser is imaged onto a CCD camera. The CCD camera is capable of obtaining two images with 4 bit resolution, which is sufficient for centroid location of the particles in the two laser sheet illumination. The two images are cross-correlated to obtain the velocity. Thus the procedure does not require a scanning mirror biasing device, which seriously impacted the dynamic range and the accuracy of past PIV systems. The digital image is processed using cross-correlation software to yield the maximum spatial frequency and the resulting velocity.

### UCI DoE Testing of Swirl cups

Several features of swirl cups, Figure 16, are critical from designers' point of view including purge slots, primary and secondary swirlers (vane angles, number of vanes, vane solidity, thickness, and contours; details of the passages downstream of the vanes), mixing region between the two swirling streams, expansion rate as determined by flare angle.

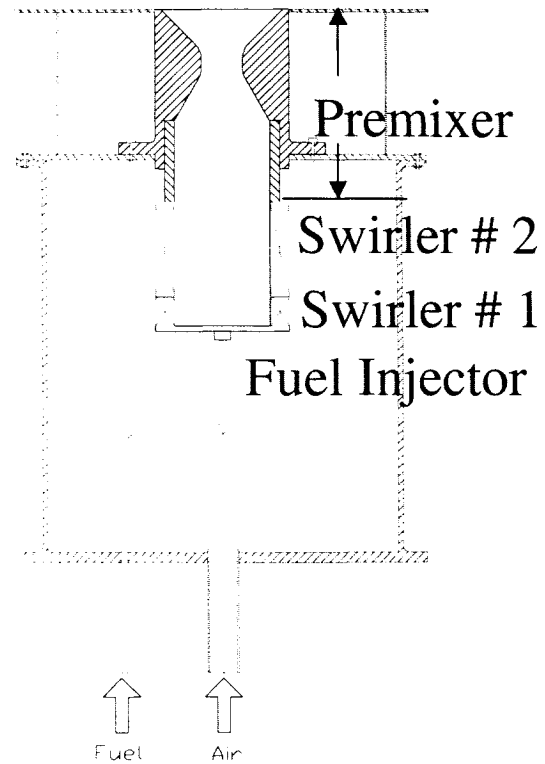


Figure 15: Purdue mixer consisting of two radial in-flow swirlers surrounding an injector followed by a premixer.

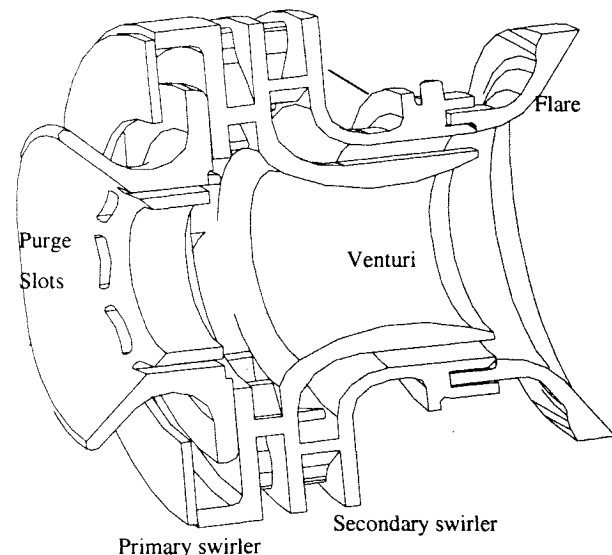


Figure 16: Typical radial/radial swirl cup

McDonnell and Samuelsen investigated the following features of swirl cup under the AFOSR Focused Research Initiative (Reference 16):

1. Primary swirler vane angles: 25, 35 and 45 deg.
2. Secondary swirler vane angles: 55, 65 and 75 deg.
3. Co- and counter-rotating primary/secondary swirlers
4. Two different fuel nozzle flow numbers ( 2.0 PPH/(psi)0.5 w/ 800 spray angle, 2.5 w/ 900 spray)
5. Nozzle tip w/ and w/o cooling (purge) air
6. With venturi or no-venturi

Figure 17 gives a snap-shot of the hardware used by the UCI combustion group.

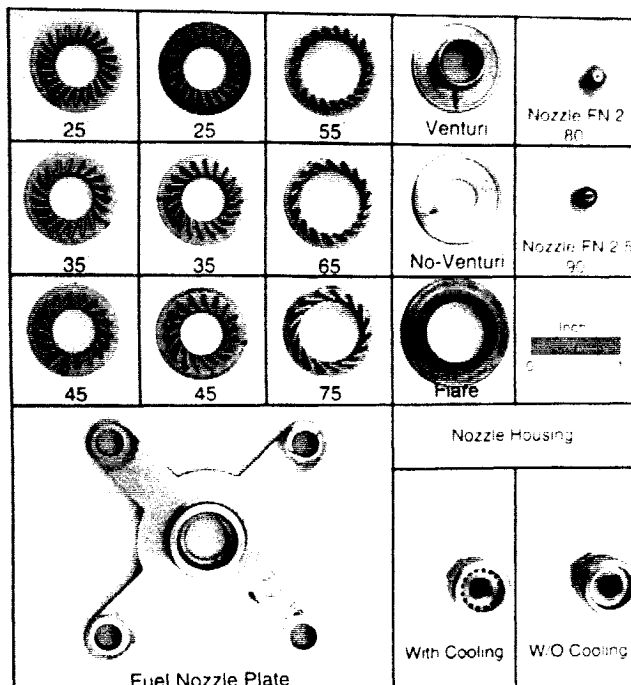


Figure 17: Swirl cup subcomponents tested under FRI sponsorship by Samuelsen and McDonnell including co-rotating and counter-rotating radial in-flow swirlers with no no-venturi.

Both the Purdue and UCI fundamental investigations compliment the combustion designers empirical design know-how as we discuss the findings reported by these two groups in the following paragraphs.

Ji and Gore<sup>21</sup> studied their set-up for the operating conditions listed below:

#### Operating Conditions

Swirler	Single Swirler	Co-Rotating Double Swirlers	Counter-Rotating Double Swirlers
Vane Angle	21°	21°	21°
Pressure Drop	2.5 %	2.5 %	2.5 %
Air Flow Rate (m <sup>3</sup> /s)	0.0292	0.0358	0.0442

The velocity vectors averaged over 200 frames are plotted with a color code indicating the speed in the right half and the vorticity in the left half in Figures 18-20.

The flow field at the exit of all three premixers depicts the central recirculation zone and the strong annular flow separated by a conical annulus of stagnant mean flow. The flow field of the single swirler (Figure 18) and the co-rotating double swirlers (Figure 19) are very similar to each other except for the scaling up of the total flow rate for the fixed pressure drop.

However, the counter-rotating double swirler generated flow field shown in Figure 20 has a weaker reverse flow into the nozzle near the axis. Further, the recirculation zone is shorter and the conical stagnation region annulus is much thinner near the nozzle exit. The vorticity has a higher magnitude but is restricted to a narrower and shorter region for the counter-rotating double swirler. Since the flame stabilization and flame structure are related with the vorticity characteristics in addition to the low-velocity regions, one could infer indirectly that these mixers should have different emissions and lean blowout performance.

Based on these images, it is clear that the flow field of practical double swirlers is significantly different from that of single swirlers used in generic laboratory experiments. Therefore, attention is necessary for improved understanding of interacting swirling flows used in practice. Moreover, if one is studying double swirlers with interdependent liquid spray formation processes, the resulting output might be even more complex as illustrated by the UCI work16.

Planar Laser Liquid-Induced Fluorescence (PLLIF) was employed to characterize the planar distribution of fuel downstream of the mixer. A total of 32 images of the fuel spray were captured and averaged for the analyses conducted. The spray distributions for two fuel injectors (w/ 0.5 and 1.35 PPH/(psi)0.5) were compared for four different swirler geometry configurations (i) 35/65/Counter-Swirl/With Venturi, (ii) 25/55/Co-Swirl/With Venturi, (iii) 45/55/Co-Swirl/Without Venturi, and (iv) 45/55/Counterwirl/With Venturi. In each case, a 4% pressure loss was set for the air flow. The PLLIF images collected are shown in Figure 21.

The results revealed that changes in flow number from 0.5 to 1.35 have little impact on the fuel distribution produced. It was also later observed (not shown in the present results) that the lean stability limit was also not affected strongly by nozzle flow number or spray angle. Since the injector appeared to play a small role in the performance of the system, this allowed this parameter to be dropped from the list of variables, thereby allowing more time for other types of experiments.

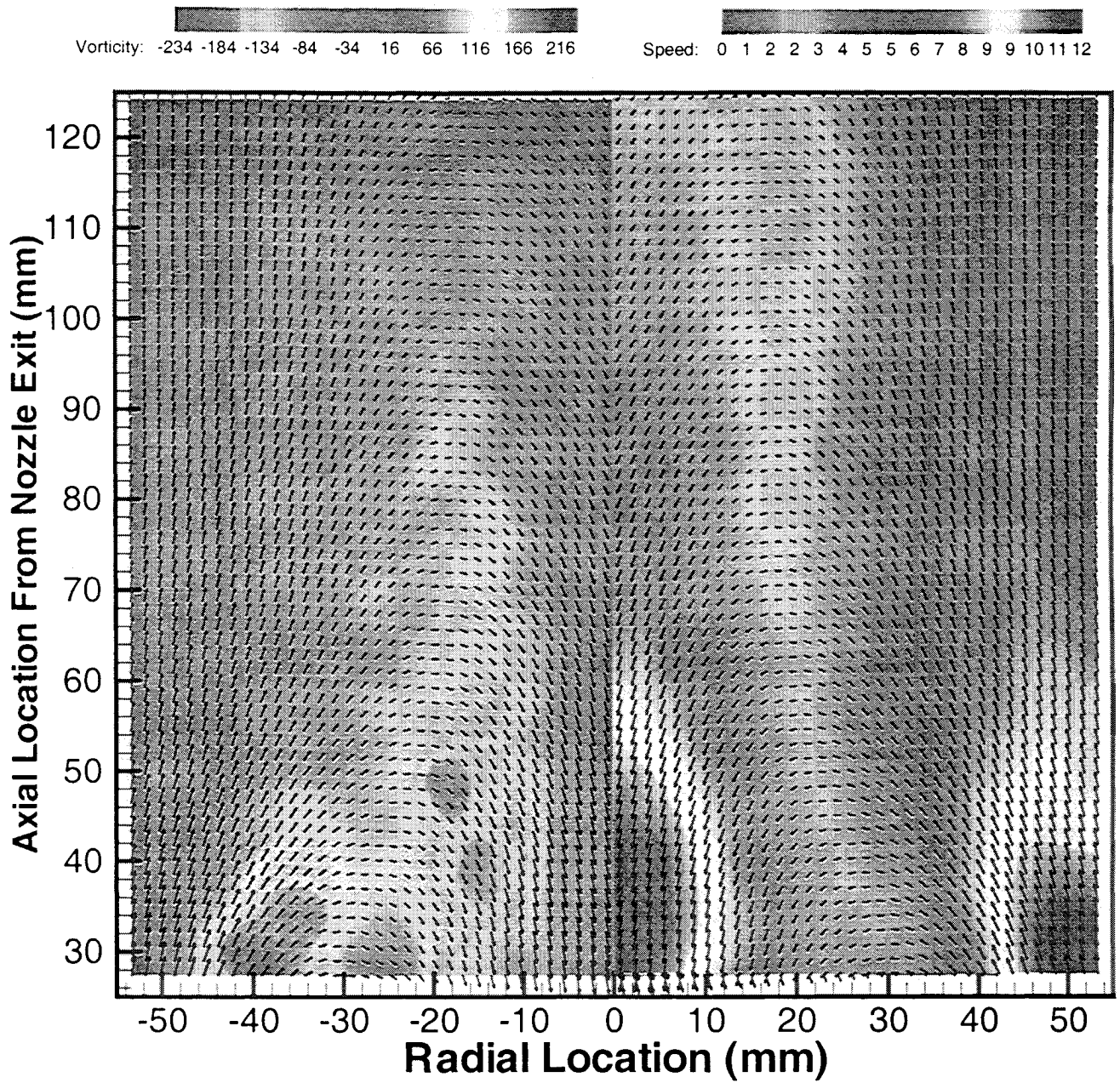


Figure 18: Velocity vectors downstream of the mixer exit for a single swirler assembly with speed (right) and vorticity (left) shown in the color code.

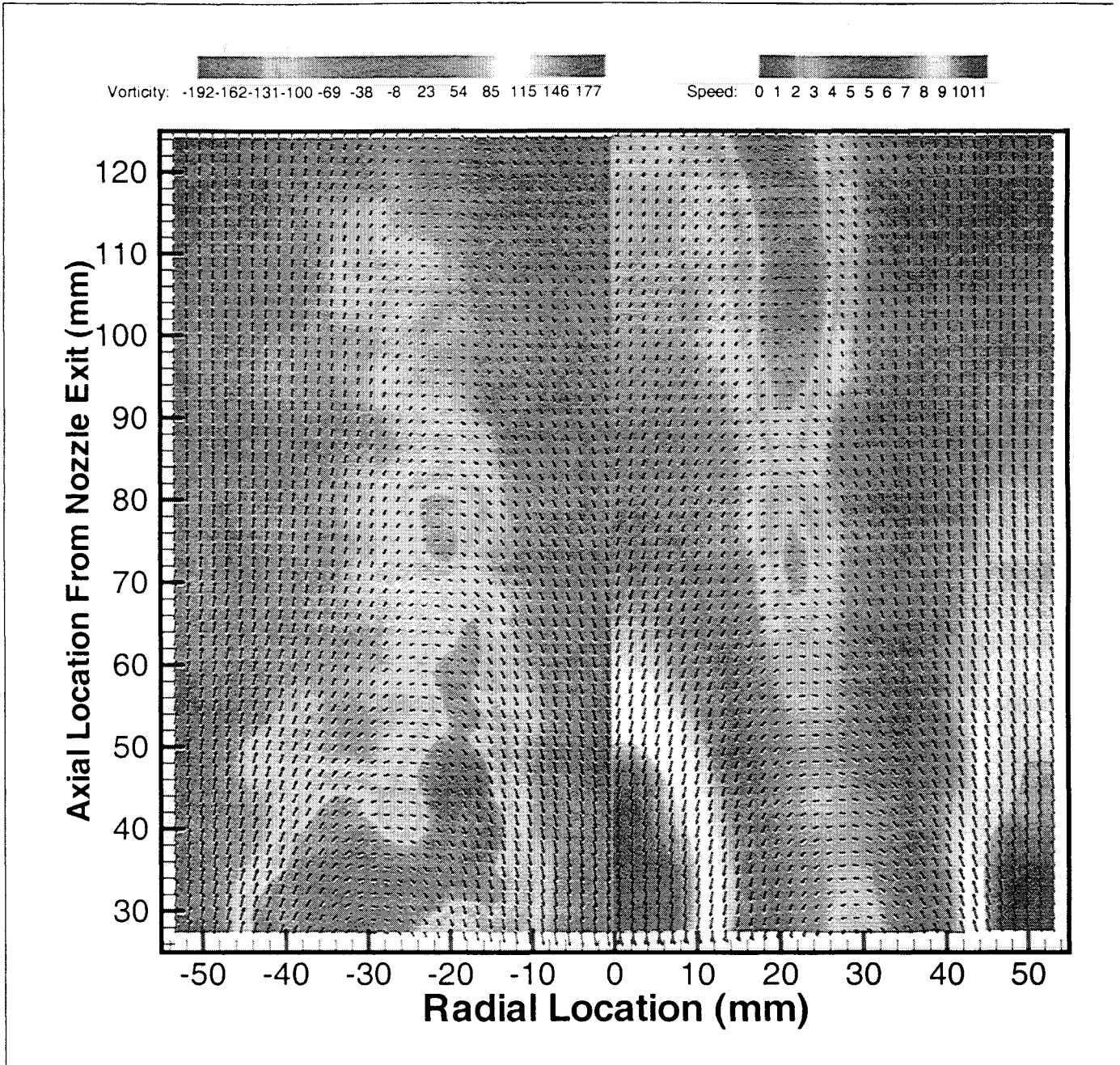


Figure 19: Velocity vectors downstream of the mixer exit for a co-rotating double swirler assembly with speed (right) and vorticity (left) shown in the color code.

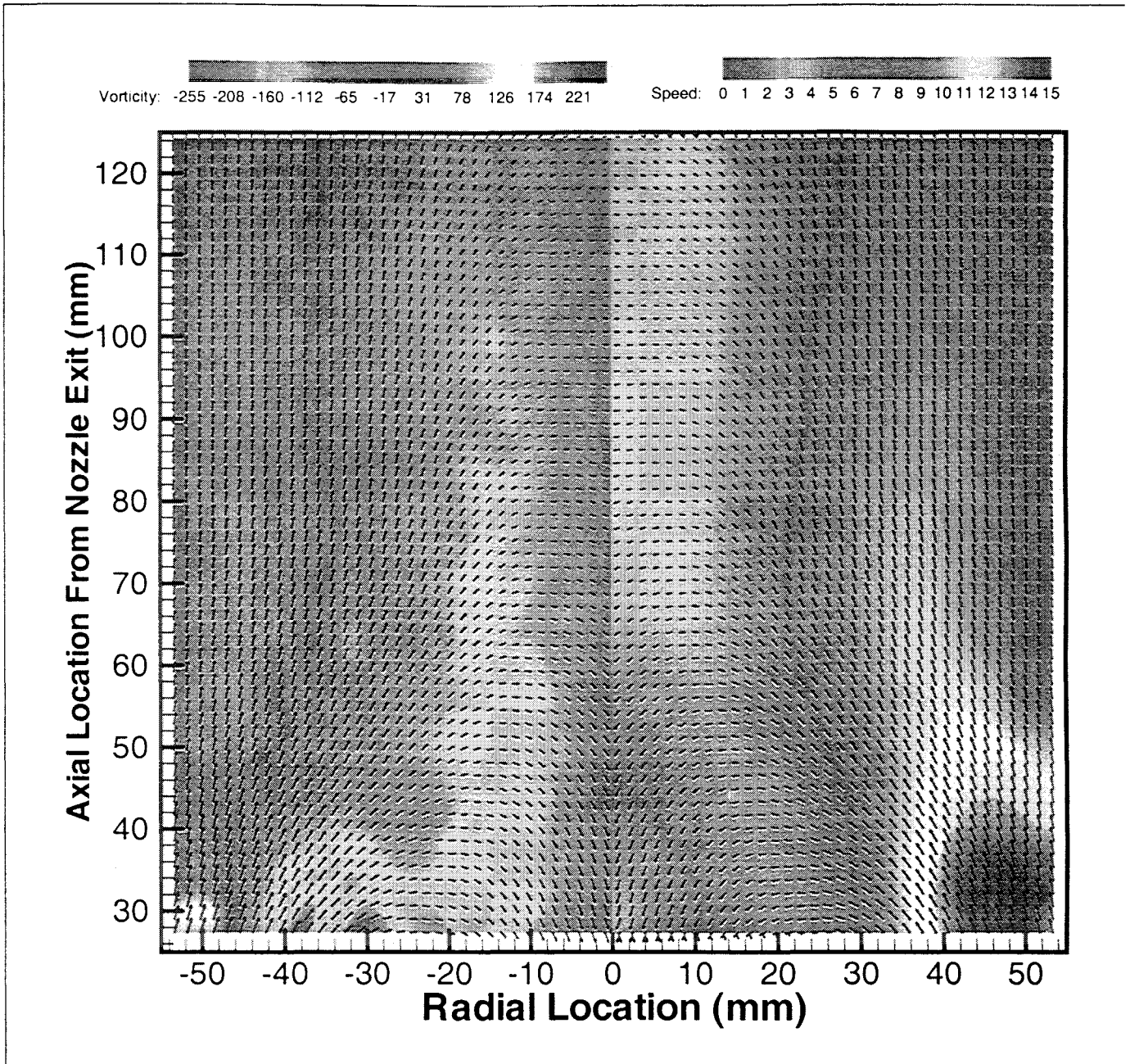


Figure 20: Velocity vectors downstream of the mixer exit for a counter rotating double-swirler assembly with speed (right) and vorticity (left) shown in the color code.

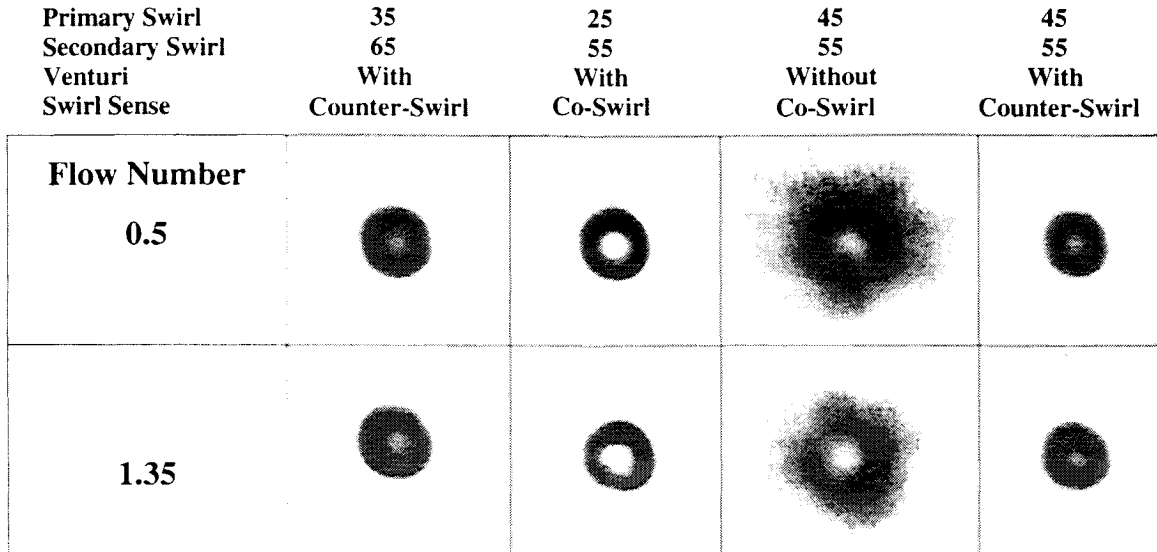


Figure 21: Comparison of Fuel Distribution with Two Fuel Nozzles (FN=0.5 and 1.35) as impacted by swirlers arrangement (co- and counter-swirl direction) w/ and w/o venturi.

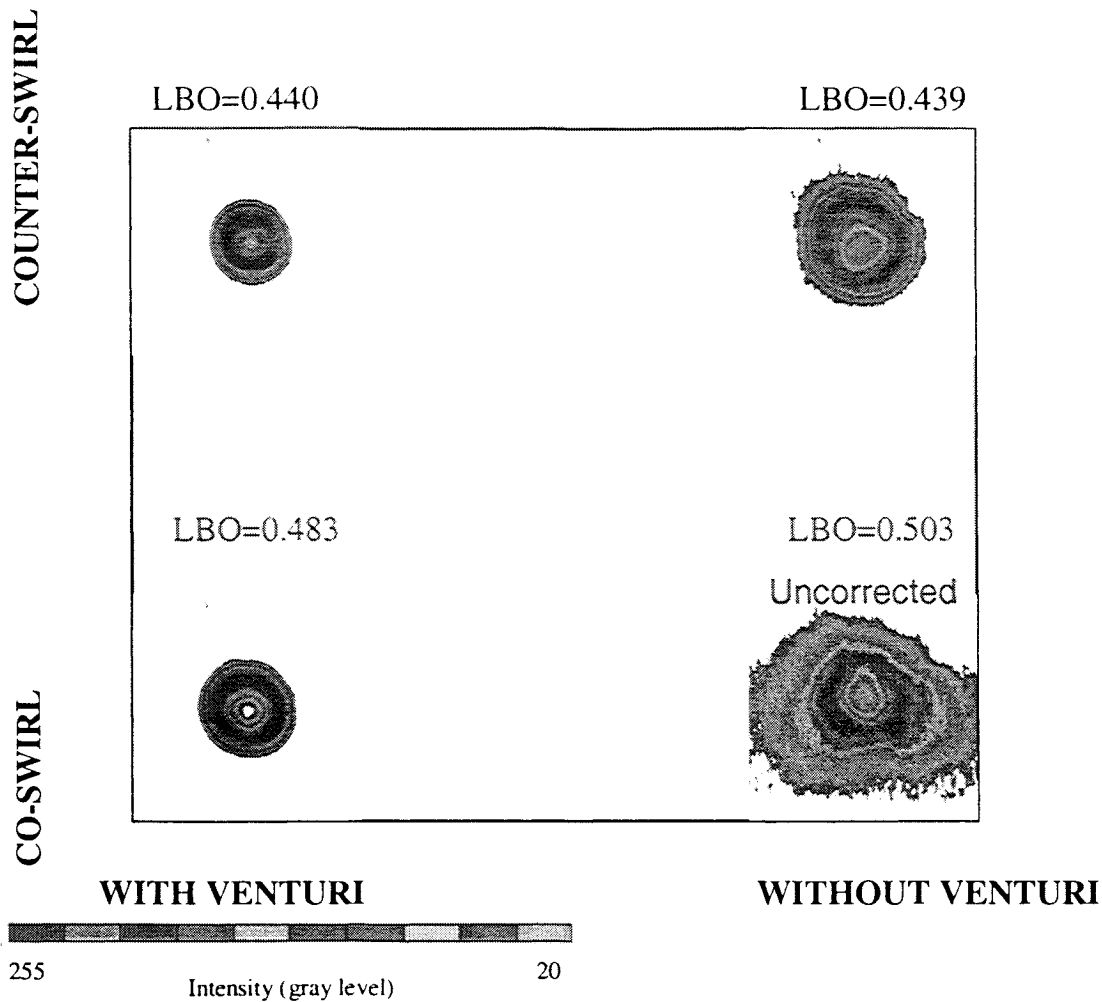


Figure 22: Effect of Venturi and Swirl Sense on Spray Distribution [Primary Swirl 35°, Secondary Swirl 65°.

A parametric investigation was conducted on the swirl cup configurations under non-reacting conditions to identify the key factors affecting the fuel distribution. The fuel distribution was compared for all the configurations at 25 mm downstream of the exit plane of the mixer to quantify the impact of 1) the swirl sense, 2) the primary and the secondary swirl vane angle, 3) with or without the presence of venturi. The presence of venturi consistently reduces the spread of the fuel spray. The co-swirl creates a larger spray area than does counter swirl. The swirl strength has no impact on the fuel distribution. This is a surprising result given the range of swirl strengths considered for both the primary and secondary swirlers. This results implies that either (1) the range of swirl strength is not wide enough to reveal an effect given the impact of venturi and swirl sense or (2) the swirl angle is not a good indicator of the actual swirl strength. This observation is worth of further study. Regardless, for the purpose of this program, the results reveal that the venturi and swirl sense are the only two important factors, which dictate fuel distribution.

Based on fuel distribution, swirl sense and presence of the venturi were identified as being of most importance to study in more detail in the comprehensive measurements. Figure 22 shows typical example for the measured spray distribution with 35°/65° primary/secondary swirlers package for co- and counter-swirl swirl cups with and without venturi. Clearly, the spray distributions are quite different for the four configurations. But what is surprising is that the maximum to minimum LBO equivalence ratio is only 1.15.

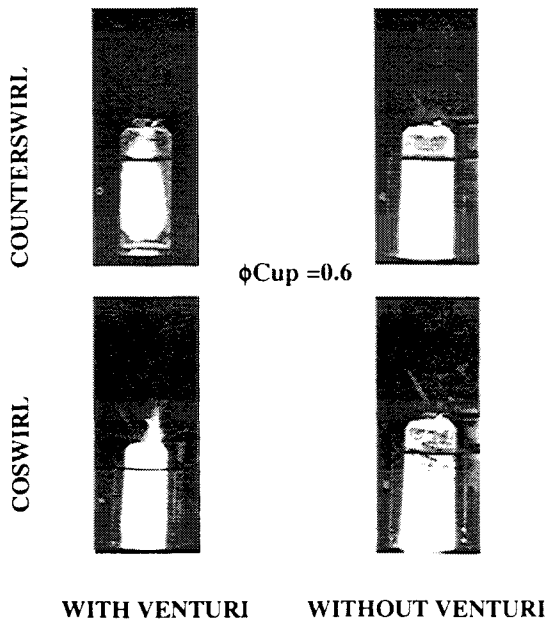


Figure 23: Flame structure at 0.6 swirl cup equivalence ratio as impacted by swirl direction with and without venturi.

Another interesting experimental observation is how different are the flame structures for the selected four configurations for a given swirl cup equivalence ratio (e.g., 0.6, as shown Figure 23) or just before lean blow-out as indicated in Figure 24. In both of these figures, the swirl cups are located at the bottom, and the flow is from bottom to the top of the figure.

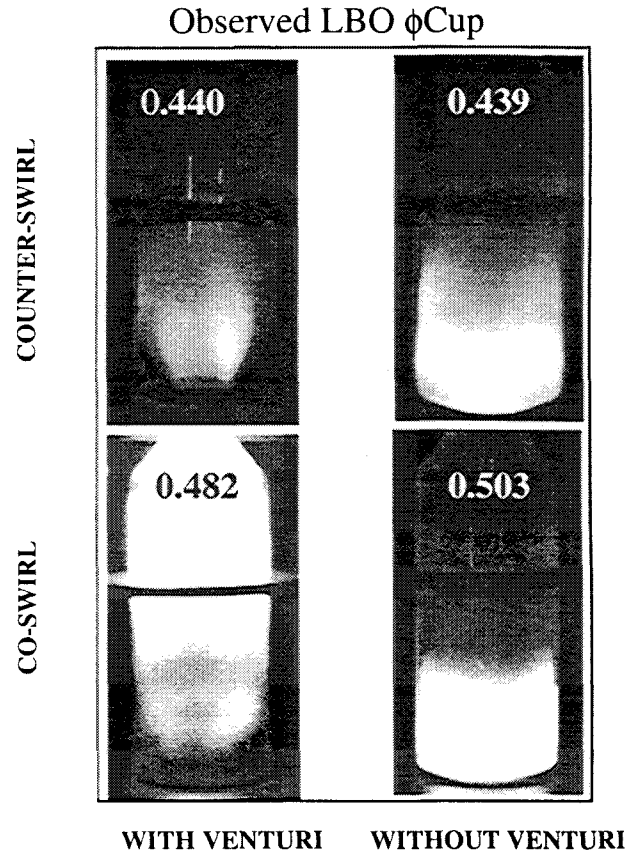


Figure 24: Flame structures just before lean flameout and the corresponding swirl cup LBO equivalence ratios.

These swirl cup results from UCI's combustion group and the nonreacting flow measurements from Ji and Gore<sup>21</sup> clearly show the challenge for the RAMA design tools and the need for developing LES-based models for production swirl cup-based combustors in addition to the DLE combustion system as discussed in Section 4.

### VI. UC and NRL Fundamental Studies

The triple annular research swirlers (TARS) based injector followed by combustor mounted swirlers (as shown typically by the four-swirler arrangement in Figure 6 are considered a challenging candidate for conducting future combustion research. TARS can have different arrangement of swirlers in regard to vane angles, direction of rotation, area flow splits, details on the flow passages downstream of the vane packages. It can have easily at

least three fuel injectors, namely axial injector along the center-line, and two sets of cross-stream injection. One can make any one or multiple of the three injection devices modulate the fuel flow to study the effect of active combustion control on combustor performance, operability and emissions.

Gutmark, Grinstein and their colleagues are conducting experimental and analytical investigation<sup>20</sup> on TARS provided by BFGoodrich Aerospace. Gutmark has set up a combustion research test rig at University of Cincinnati to parametrically evaluate the design features of TARS as shown in Figure 25. The combustor rig features multiple independent fuel supply lines for efficient fuel distribution and multiple air inlets to obtain co- and counter rotating swirling air streams. The entire combustion air is supplied through the mixer/fuel injector, which is located at the combustor dome. The mixer includes three air passages equipped with swirlers lead into the combustion chamber. The two central coaxial passages feature axial swirlers while the external air passage has radial swirling vanes. Air blast fuel atomizers are distributed between the second and third annuli. Fuel is injected into the inner and outer annuli for efficient mixing. A conventional pressure atomized pilot is located in the central passage.

A conventional pressure atomized pilot is located in the central passage. The location of the fuel injector relative to the sudden expansion at the entrance to the combustion chamber can be varied. The length and exit nozzle of the combustor is variable to allow change in the acoustical boundary conditions, thus enabling excitation of various instability modes. The combustor is retrofitted with quartz windows to allow optical access for Particle Imaging Velocimetry (PIV), Laser Doppler Velocimeter (LDV) and Phase Doppler Particle Analyzer (PDPA) for droplet size and velocity measurements.

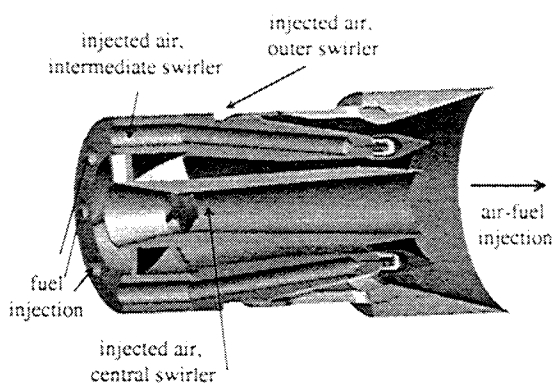


Figure 25: Triple Annular Research Swirler (TARS) mixer being studied by UC and NRL.

A stereoscopic Particle Imaging Velocimetry (PIV) system was used to map the flow field exiting the fuel injector. The three mean and turbulent velocity components were measured simultaneously. Two-component PDPA system

was used to map the flow field at the exit from the fuel injector and obtain time resolved data as well as measure the dispersion pattern of the simulated injected fuel.

As explained by Grinstein et al<sup>20</sup>, one needs to develop a reliable and defensible strategy for calculating or specifying boundary conditions for the various inlets. One may be able to get away with simplifying assumption for the RAMA based calculations. However, this task is critically important for the large eddy simulations, LES. Grinstein et al<sup>20</sup> have explained this in their paper. Here, we will give a brief description. There are basically two ways of specifying the boundary conditions for the inlets – through experimental measurements or analytical calculations.

Figure 26 shows, for example, through the vane calculations as given by GEAE's Advanced Combustion Code, ACC, how complex the flow field is and its time-unsteady variations need to be specified to carry out LES.

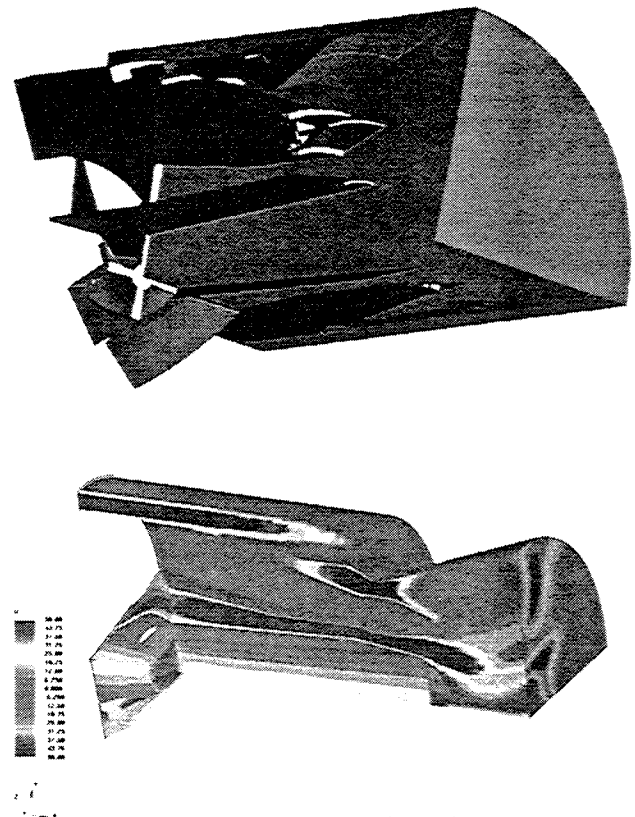
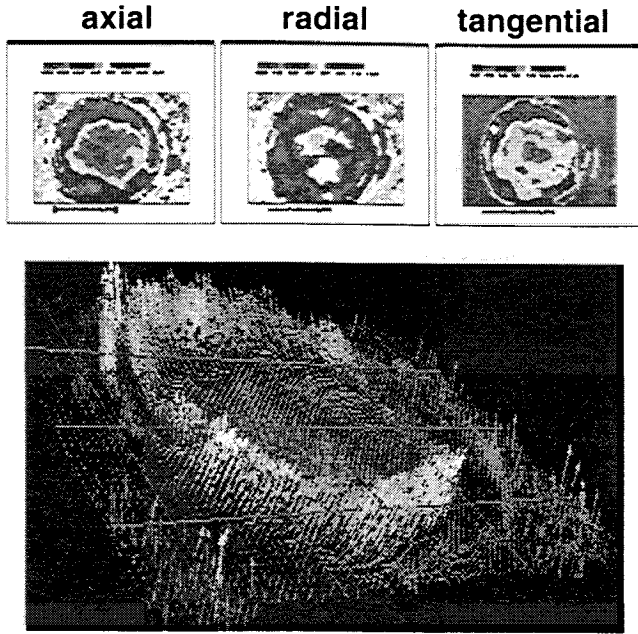
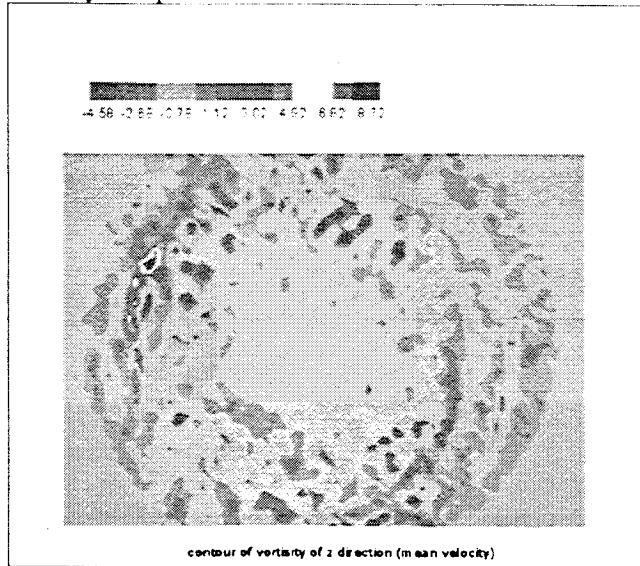


Figure 26: Through-the-vanes calculations provide the inlet conditions for the Large-Eddy Simulation.

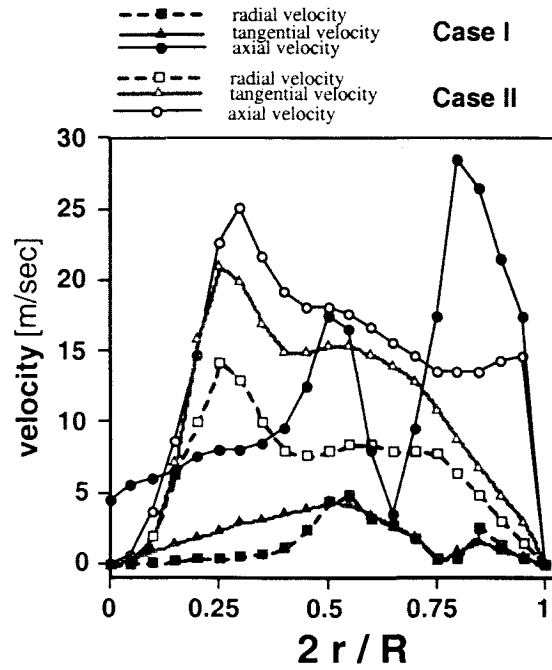
Gutmark's measurements immediately downstream of TARS, as shown in Figure 27 for one of the configurations tested can also be used for providing the inlet conditions for LES. Grinstein et al<sup>20</sup> used the both approaches as an illustration for studying the impact of inlet conditions on the LES computed flow-field.



Velocity at triple annular research swirler outlet



Axial vorticity contours at fuel injector exit  
Figure 27: Inlet conditions as measured by Gutmark downstream of the TARS mixer.



(a) Circumferentially- and time-averaged velocity profiles at the TARS outlet plane

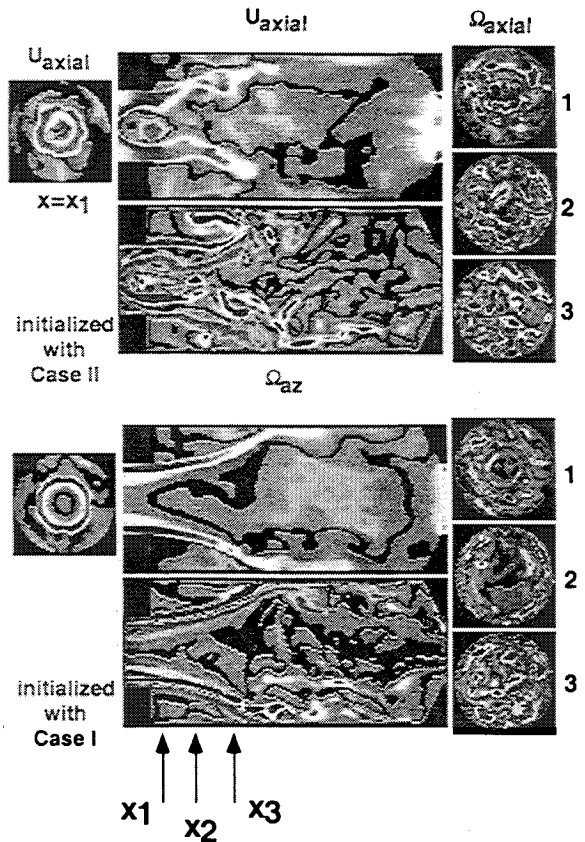


Figure 28: LES calculations by Grinstein as impacted by inlet conditions for the two configurations, identified as Case I and Case II20.

## VII. Proposal for Future Studies

Through various examples covered in the last five sections and cited references, we conclude:

1. Modern combustors (swirl cup-based recently certified propulsion engine combustors; DLE's and emerging combustor technology combustors including TAPS and TVC<sup>22</sup>) have evolved with complex fuel/air mixers to varying degree of complexity.
2. Even though the simple mixers of old-generation gas turbine combustors might have complex flow field characteristics some what similar to modern mixers, they are sufficiently different to undertake a concerted, focused research effort involving both the research community and combustion designers if we were to achieve objective listed under (6).
3. Current Reynolds averaged modeling approach (RAMA) used by combustion designers and available in commercial CFD packages is essentially an extension of "old" formulations that are not expected to give the accuracy level required as "pre-diction" design tools. Consequently, combustion design process will continue to depend heavily on iterative testing/anchoring process, which can at best give a sub-optimum combustion system in a schedule-driven design environment.
4. Experimental and CFD capabilities have developed extensively through the years that they are ready for "real design" application as discussed by the GEAE Gas Turbine Combustion Symposium participants, as summarized by Mongia<sup>23</sup>.
5. If we want to achieve the objective listed under (6), we need to develop design tools, conduct the required research (experimental, modeling), small and large scale model verification for each class of combustors which are conveniently divided into swirl cup, DLE, TAPS and TVC for GEAE combustors of significant interest.
6. Develop combustor analytical design process and tools that designers can use to design an optimum combustion systems and stand up with 85% confidence level that the predicted performance, emissions, operability and liner wall temperature levels would fall within one standard deviation ( $\sigma$ ) of the engine experimental data. The estimated values for modern propulsion gas turbine engines are:  
Landing-takeoff (LTO) NOx: 1.5 or 3.1%  
LTO CO: 2.95 or 5.0%  
LTO HC: 0.81 or 10.7%  
Max smoke number: 1.24 or 13.6%  
Liner temperature: 25<sup>o</sup>F  
Lean blowout f/a: 0.0005  
Pattern Factor: 0.03  
Temperature profile: 0.01

A two-day workshop was held in Cincinnati on April 23, 24, 2001, that included approximately 100 participants from research and design community to discuss what needs to be done to achieve the objective listed under (6). The key findings and summary of the workshop as relevant to the four combustor designs are given in Reference 23.

## VIII. Summary

Several examples have been used to illustrate mutually useful interaction between the combustion designers and the research community. Both experimental and modeling efforts have clearly shown:

- Highly complex interacting processes taking place in modern fuel/air mixing devices that are unique and distinct
- Many of these processes lead one to surmise the urgent need to formulate and validate (through extensive advanced diagnostics based database under full-scale realistic operating conditions) design-specific combustion models if one were to achieve the following accuracy objectives

In order to meet the next-generation combustion design challenges, we need to step up for developing and validating accurate analytical design tools. This will result in replacing the current empirical/analytical methodology or their recent variants, hybrid or anchored so that an optimum combustion system can be developed without intermediate-step testing required by current practice.

## REFERENCES

1. Mongia, H. C., 2001, "A Synopsis of Gas Turbine Combustor Design Methodology Evolution of Last 25 Years", ISABE 2001 Conference.
2. Mongia, H. C., 2001, "Gas Turbine Combustor Liner Wall Temperature Calculation Methodology", AIAA Paper 2001-3267.
3. Mongia, H. C., and Smith, K. F., 1978, "An Empirical/Analytical Design Methodology for Gas Turbine Combustors", AIAA Paper 78-998.
4. Reynolds, R. S., Kuhn, T. E., and Mongia, H. C., 1977, "An Advanced Combustor Analytical Design Procedure and its Application in the Design and Development Testing of a Premix/Prevaporized Combustion System", Spring Technical Meeting of the Central States Section of The Combustion Institute, March 28-30, 1977.
5. Bruce, T. W., Mongia, H. C., and Reynolds, R. S., 1979, "Combustor Design Criteria Validation Volume I, Element Tests and Model Validation", USARTL-TR-78-55A.
6. Mongia, H. C., Reynolds, R. S., and Srinivasan, R., 1984, "Multidimensional Turbulent Combustion: Analysis, Applications and Limitations", AIAA Paper 84-0477.

7. Srinivasan, R., Reynolds, R. S., Ball, I., Berry, R., Johnson, K., and Mongia, H., 1983, "Aerothermal Modeling Program Phase I Final Report" NASA CR-168243.
8. Mongia, H. C., Reynolds, R. S., and Srinivasan, R., 1986, "Multidimensional Turbulent Combustion: Analysis, Applications and Limitations", AIAA J., V24, n6, pp. 890-904.
9. Nikjooy, M., Mongia, H. C., McDonell, V. G., and Samuelsen, G. S., 1993, "Fuel Injector – Air Swirl Characterization Aerothermal Modeling Phase II Final Report – Volumes I & II", NASA CR 189193.
10. Nikjooy, M., Mongia, H. C., Sullivan, J. P., and Murthy, S. N. B., 1993, "Flow Interaction Experiment Aerothermal Modeling Phase II Final Report – Volumes I & II", NASA CR 189192.
11. Sanborn, J. W., Lenertz, J. E., and Johnson, J. D., 1987, "Design and Test Verification of a Combustion System for an Advanced Turbofan Engine," AIAA Paper 87-1826.
12. Mongia, H., Al-Roub, M., Danis, A., Jeng, S.-M., Johnson, A., McDonell, V., and Samuelsen, G. S., Vise, S., 2001, "Swirl cup Modeling," AIAA Paper 2001-3576.
13. Joshi, Narendra D., Mongia, Hukam C., Leonard, Gary Stegmaier, Jim W., and Vickers, Ed. C., 1998, "Dry Low Emissions Combustor Development," ASME-98GT-310.
14. Mongia, H. C., Coleman, E. B., and Bruce, T. W., 1981, "Design and testing of two variable geometry combustors for high altitude propulsion engines", AIAA Paper 81-1389.
15. Sanborn, J. W., Mongia, H. C., and Kidwell, J. R., 1983, "Design of a low-emission combustor for an automotive gas turbine", AIAA Paper 83-0338.
16. Mongia, H., Peters, J., Lucht, R., Dibble, R., Chen, J.-Y., Menon, S., Bellan, J., Samuelsen, G., McDonell, V., Santoro, R., Santavicca, D., and Ghoniem, A., 1999, "AFOSR Focused Research Initiative: Low-Emissions, High- Performance Gas Turbine Engines",
17. Lefebvre, Arthur H., 1999, "Gas Turbine Combustion", Taylor & Francis, Chapter
18. Kim, W-W. Menon, S., and Mongia, H.C. , *Combust.Sci. and Tech.*, **143**, 25 (1999).
19. Sankaran, V., and Menon, S., 2001, "Computational Modeling of Mixing, Combustion and Control in Turbulent Swirling Flows," AIAA Paper 2001-3426.
20. Grinstein, F. F., Young, T. R., Li, G., Gutmark, E. J., Hsiao, G., and Mongia, H. C., 2001, "Flow dynamics in a swirling jet combustors," Turbulent Shear Flow Conference.
21. Ji, J., and Gore, J., 2001, "A Study of Pressure Oscillations Caused by Swirling Combustion in an Advanced Turbine System (ATS) Premixer Module," AIAA Paper 2001-3849.
22. Roquemore, W. M., Dale Shouse, Dave Burrus, Art Johnson<sup>1</sup>, Clayton Cooper, Beverly Duncan , K.-Y. Hsu, V. R. Katta, G. J. Sturgess, and Illari Vihinen, 2001, "Trapped Vortex Combustor Concept for Gas Turbine Engines," AIAA-2001-0483.
23. Mongia, Hukam. C., 2001, "Summary of GEAE Gas Turbine Combustion Technology & Research Symposium, April 23, 24, 2001."